REFERENCE 16

H. C. PAXTON, "FAST CRITICAL EXPERIMENTS," IN PROGRESS IN NUCLEAR ENERGY (PERGAMON PRESS, LTD., 1981), VOL. 7, PP. 151-174.

Progress in Nuclear Energy, Vol. 7, pp. 151–174
Pergamon Press Ltd., 1981. Printed in Great Britain

0079 6530/81/0701-0151 $05.00/0

FAST CRITICAL EXPERIMENTS

HUGH C. PAXTON

University of California, Los Alamos National Laboratory, Los Alamos, New Mexico 87545, U.S.A.

(*Received* 10 *December* 1980)

1. INTRODUCTION

The history of fast-neutron critical assemblies falls into three overlapping phases. The first, beginning in 1948, relates to simple, compact metal assemblies with extremely high-energy neutron spectra. Critical parameters were directed initially toward checking cross-section sets used in nuclear weapon calculations, but are also applicable to parameters controlling the higher-energy portions of fast-reactor spectra.

The second phase, starting 6 yr later, covers larger, more diffuse assemblies that are still simply describable because of uniform core and reflector regions. At first directed toward checking basic calculations applicable to small fast reactors, members of this class have increased in size throughout the years, with progressively softer spectra keeping pace with growing concepts of fast reactors.

The final phase, starting in 1955 but assuming primary importance in the 1970s, applies to engineering mockups with the structural perturbations of practical fast power reactors. Simulated control elements, for example, introduce non-uniformities that complicate the description of these assemblies. No longer suitable for checking general cross-section sets, these assemblies instead provide guidance for the special computational techniques required for large perturbations and severe discontinuities in composition.

This account will emphasize applications of experimental data from the first two categories that encompass the so-called 'benchmark' assemblies. Descriptions of these assemblies are idealized by means of generally small corrections to simple geometry and to homogeneous core and reflector regions. The idealized critical specifications and other integral parameters, such as those characterizing neutron spectra, reactivity coefficients, and prompt-neutron decay constants, then supplement differential data to guide the refinement of cross-section sets.

2. SMALL VERY-FAST METAL ASSEMBLIES

The earliest fast assemblies, those of compact metal, were designed with spherical (or near-spherical) symmetry to make them amenable to the one-dimensional computational techniques that were practical at the time. Most of these assemblies were at the Los Alamos National Laboratory.

2.1. *TOPSY and early measurements*

This program began with TOPSY, a machine accommodating enriched-uranium cores with thick natural-uranium or nickel reflectors[1]. To maintain flexibility in those days of uncertain critical sizes, the cores were constructed of blocks with dimensions as small as ½ in. Thus spheres were approximated by ½ in. steps across the surface. There were U(94)* cores at full density and with distributed ½ in. cubic voids to decrease average densities by as much as one half. Similarly, distributed ½ in. cubes of natural uranium reduced average ^{235}U concentrations to as little as 47.3%. When a spherical assembly of U(93) in natural uranium became available in 1958 (a FLATTOP assembly), TOPSY was retired[2].

In the meantime, techniques for measuring the significant neutronic characteristics of fast assemblies were being tested in TOPSY with varying degrees of success. We discuss these tests more for the sake of background than for the immediate value of results.

2.1.1. *Reactivity contributions.* TOPSY's stacked-block structure did not lead to the precise reproducibility desired for measuring perturbations introduced by hand, and the core was too small for remote introduction of perturbing samples by mechanisms that became known as 'reactivity oscillators' when later applied so successfully to larger systems. It was only with difficulty and much wasted

* U(x) means uranium containing x wt% ^{235}U.

effort that there resulted a reasonably satisfactory survey of reactivity contributions of many materials as functions of radius[3]. Corrections to zero-size 'reactivity coefficients' were confirmed by varying the sizes of some perturbing samples. Results for ^{235}U and ^{238}U (of the many materials surveyed) provided corrections to idealized spherical geometry.

2.1.2. *Reaction rates*[4]. Several techniques for measuring reaction rates were tested by means of detectors embedded in a hole introduced into the TOPSY core. Beta activities from the reactions $^{197}Au(n,\gamma)$ and $^{32}S(n,p)$ were measured satisfactorily by means of a methane-flow proportional counter. The low-energy gold detector was calibrated by irradiation in a thermal column where the cross section was known, and the threshold sulfur detector by high-energy activation and use of a cross section that had been measured. Later, this general technique was extended to the high-energy reactions $^{31}P(n,p)$, $^{27}Al(n,p)$, $^{56}Fe(n,p)$, $^{27}Al(n,\alpha)$, $^{63}Cu(n,2n)$ and $^{63}Cu(n,\gamma)$, and to a general survey of low-energy reactions[5-8].

One of the methods explored for measuring reaction rates of fissionable materials, though appealing in principle, did not work out in practice. This made use of a fission-product 'catcher', a foil in contact with irradiated fissionable material, which collected recoiled fission products for measurement in a methane-flow counter. This was to eliminate background from natural radioactivity, from reactions competing with fission, and from prior irradiations, but results remained inconsistent, presumably because a transfer of sample corrosion products to the catcher could not be prevented. Although abandoned at the time, a modification of this technique, revived at Winfreth, uses a solid-state track recorder as both catcher and detector[9].

For ^{235}U and ^{238}U, it turned out that background did not interfere with the interpretation of fission-product γ-activity as measured by a NaI(Tl)-photomultiplier scintillation counter. Nevertheless this scheme became obsolete with the development of small, multiple fission chambers, supplemented by radiochemical analyses. The first chamber of this type contained two back-to-back replaceable foils, each with a deposit of fissionable material[4]. The housing was 1 in. long and $\frac{7}{8}$ in. in diameter. With the chamber embedded in operating TOPSY, fission-pulse rates from pairs of the following could be compared directly: ^{233}U, ^{234}U, ^{235}U, ^{236}U, ^{238}U, ^{237}Np and ^{239}Pu. Weights of foils were determined after-the-fact by thermal fission counting or by α-counting in standardized geometry, and confirmed by fluorometric analyses. This back-to-back chamber was succeeded by smaller ($\frac{1}{2}$ in. equilateral) 'four-barrel' chambers, each containing four tiny cylindrical foils with fissionable deposits. In these, and similar chambers used elsewhere, ^{240}Pu and ^{241}Pu have been added to the above list of fissionable isotopes.

In addition to calibration of fissionable deposits, radiochemical analyses established numbers of activations in irradiated foils directly. Fission data were given by analysis for the fission product ^{99}Mo, the 2.3 day β-activity of ^{239}Np was a measure of ^{238}U capture, and the 6.8 day β-activity of ^{237}U similarly was a measure of $^{238}U(n,2n)$. To this day, refined radio-chemical analyses are used wherever fast assemblies exist.

2.1.3. *Spectral indexes*. The earliest quantities for characterizing internal neutron spectra, ratios of effective fission cross sections or activation cross sections, are still valued as computational check-points[10]. As determined by measurements discussed above, fission ratios such as $\bar{\sigma}_f(^{238}U)/\bar{\sigma}_f(^{235}U)$ and $\bar{\sigma}_f(^{238}U)/\bar{\sigma}_f(^{237}Np)$ broadly characterize spectra, $\bar{\sigma}_f(^{233}U)/\bar{\sigma}_f(^{235}U)$ and $\bar{\sigma}_f(^{239}Pu)/\bar{\sigma}_f(^{235}U)$ add low-energy information, and ratios of $\bar{\sigma}_{n,p}(^{31}P)$ to $\bar{\sigma}_{n,p}(^{27}Al)$ and $\bar{\sigma}_{n,p}(^{56}Fe)$, for example, distinguish among high-energy tails. Of course other ratios involving $\bar{\sigma}_f(^{240}Pu)$, $\bar{\sigma}_{n,\gamma}(^{238}U)$, $\bar{\sigma}_{n,\alpha}(^{27}Al)$, $\bar{\sigma}_{n,2n}(^{63}Cu)$ and $\bar{\sigma}_{n,\gamma}(^{63}Cu)$ add further to the spectral information

Attempts to measure a TOPSY neutron spectrum in detail were unsuccessful. Track measurement in ^{6}Li-loaded emulsions exposed internally suffered from confusing proton-recoil background. Only much later was it shown elsewhere that 'speck loading' of the ^{6}Li could unambiguously identify the disintegration tracks[11]. Further the core spectrum lost its identity in passing through an opening in the reflector for external measurement. Throughout the years, techniques developed in laboratories with larger assemblies have come to include successful extraction of core spectra for analysis by various energy-sensitive detectors and by time-of-flight discrimination[9,12]. Internal measurements by small proton-recoil chambers and ^{3}He disintegration chambers have also proven useful[13].

2.1.4. *Prompt-neutron decay constant*. The obvious method of pulsing a subcritical assembly with an external neutron source and observing the gross decay of simultaneously initiated fission chains[14] was not used with TOPSY for measuring the prompt-neutron decay constant. Instead there was applied a technique developed by Bruno Rossi, based on the self-modulation of fission chains in a near-critical assembly. These chains, random-initiated, decay on the average like a pulsed system. An internal fission

:tector to a time-scale analyzer with channels the order of a microsecond shows the expected decay of time-correlated pulses above a large uniform background. So-called 'Rossi-α' decay constants were established for reactivities that started subcritical and extended into the slightly supercritical region (of course, below prompt criticality)[15]. Subsequent improvements in time-scale analyzers have resulted largely in ease of data collection.

2.2. *Other small metal assemblies at Los Alamos*[16]

Between 1963 and 1970 other simple metal assemblies at Los Alamos were set up in the following sequence. LADY GODIVA consisted of an unreflected U(93.7) sphere with buttons fitting into surface depressions for reactivity adjustment beyond the range of two ~40-cent* control rods. Like LADY GODIVA, any assembly described as spherical has perturbing control rods and other reactivity-adjustment and mounting features that require correction to a uniform sphere by means of measured reactivity coefficients. In the absence of reflector, it was possible to measure the LADY GODIVA leakage spectrum directly by means of external proton-recoil plates[17]. Ultimately the dynamic characteristics of this assembly were confirmed by extending the reactivity slightly above prompt criticality[18]. The resulting intense fission 'bursts' proved to be useful neutron sources but did not contribute to the improvement of cross section sets.

The next assembly in this category, JEZEBEL, was basically an unreflected sphere of plutonium containing 4.5% ^{240}Pu. Later, there were mounted on the same framework spherical components of plutonium containing 20.1% ^{240}Pu, and of ^{233}U. JEZEBEL was returned to its initial composition after these temporary assemblies were surveyed. Incidentally, the survey of the ^{233}U sphere was less complete than for other assemblies because manipulation was limited by intense γ activity of ^{208}Tl that had grown into the material by decay from the impurity ^{232}U.

Spheres of the three fissile materials, but reflected by thick natural uranium, were put together on the FLATTOP assembly machine. Interchangeable cores of U(93.2), Pu and ^{233}U were fitted by means of uranium adapters into spherical uranium reflector components mounted permanently on the machine.

Of less significance as benchmarks were critical unreflected cylinders of interleaved U(93.4) and natural uranium plates with the average compositions U(53.6) and U(37.7), and a similar cylinder averaging U(16.2) but reflected by 3-in.-thick natural uranium. Critical specifications and values of Rossi-α are reliable, but the spectral indexes $\bar{\sigma}_f(^{235}\text{U})/\bar{\sigma}_f(^{238}\text{U})$ and $\bar{\sigma}_f(^{237}\text{Np})/\bar{\sigma}_f(^{238}\text{U})$ are questionable because of heterogeneity. Also, critical dimensions were extrapolated from slightly subcritical spheres of Pu in U(93.2) and ^{233}U in U(93.2), and heterogeneous cylinders averaging U(16.0), U(14.1), U(12.3) and U(10.9). The latter series of cylinders merges in size with the second category of diffuse assemblies that we shall discuss later.

Bucklings measured in exponential columns averaging U(9.18), U(6.53), U(5.14), U(4.29) and of natural uranium crossed the value zero at U(5.4)[19] This is of some historical interest in view of a fictitious assembly, 'SCHERZO 556', consisting of homogeneous U at $k_\infty = 1$, that has been proposed as a standard for checking cross-section sets. This composition, U(5.49), is based on recent measurements at Fontenay-aux-Roses, Cadarache, Karlsruhe and Winfreth (the '556' refers to 5.56 at% ^{235}U)[20]. The origin of SCHERZO 556 and of appropriate spectral indexes will be discussed later.

2.2.1. *Idealized critical characteristics.* Corrections for perturbations and other irregularities led to idealized critical specifications for selected small metal assemblies. These specifications for assemblies that attained criticality appear in Table 1, and for the spherical assemblies are translated into number densities and radii in Table 2.

Spectral-index values for bare and uranium-reflected ^{235}U, ^{233}U and Pu were analyzed for weighted averages and reliability[10,21]. The results deemed appropriate for checking calculations are listed in Table 3. The reactions that sample high-energy spectral tails, ^{31}P(n,p), ^{27}Al(n,p), ^{56}Fe(n,p), ^{27}Al(η, α) and ^{63}Cu(n, $2n$) contribute negligibly to the refinement of cross-section sets. But they have confirmed slight differences among the ^{235}U, ^{233}U and ^{239}Pu fission spectra.

Although all reactivity coefficients (corrected to zero sample size) serve in principle as check-points for cross-section sets, only the more significant are selected for display at this point. Table 4 gives central reactivity coefficients of ^{233}U, ^{235}U, ^{238}U and ^{239}Pu for the seven assemblies listed in Table 3[3,22]. Ratios of these values are also included because they are characteristics independent of critical size.

Because a prompt-neutron decay constant, α, is a function of reactivity, its value at delayed criticality, α_{dc}, may be chosen as characteristic of an assembly. Still more fundamental, though, is the prompt-neutron

* The dollar, 100 cents, is the reactivity increment between delayed and prompt criticality.

Table 1. Idealized critical specifications of simple metal assemblies

Name	Core			Reflector	Critical Mass (kg)
	Shape	Composition	Density (g/cm^3)		
LADY GODIVA	Sphere	U(93.71), 1.02 wt% ^{234}U	18.74 (U)	None	52.42 ± 0.15 (U)
FLATTOP-U(93)	Sphere	U(93.24), 1.02 wt% ^{234}U	18.62 (U)	U(nat), 19.0 g/cm^3 18.01 cm thick	17.84 ± 0.04 (U)
JEZEBEL-Pu(4.5)	Sphere	Pu(1.02 wt% Ga) 4.5 at% ^{240}Pu, 0.3 at% ^{241}Pu	15.61 (alloy)	None	17.02 ± 0.10 (alloy)
JEZEBEL-Pu(20.1)	Sphere	Pu(1.01 wt% Ga) 20.1 at% ^{240}Pu, 3.1 at% ^{241}Pu 0.4 at% ^{242}Pu	15.73 (alloy)	None	19.46 ± 0.16 (alloy)
FLATTOP-Pu	Sphere	Pu(1.01 wt% Ga) 4.80 at% ^{240}Pu, 0.30 at% ^{241}Pu	15.53 (alloy)	U(nat), 19.0 g/cm^3	6.06 ± 0.03 (alloy) 19.61 cm thick
JEZEBEL-^{233}U	Sphere	^{233}U (98.13 at%) 1.24 at% ^{234}U, 0.03 at% ^{235}U 0.60 at% ^{238}U	18.42 (U)	None	16.53 ± 0.07 (U)
FLATTOP-^{233}U[a]	Sphere	^{233}U (98.13 at%) 1.24 at% ^{234}U, 0.03 at% ^{235}U 0.60 at% ^{238}U	18.42 (U)	U(nat), 19.0 g/cm^3 19.52 cm thick	6.21 ± 0.03 (U)
JEMIMA-U(53)	Cylinder 26.7 cm dia	Repeated layers: 0.803 cm U(93.4) 0.602 cm U(nat)	18.83 (Av)	None	162.6 ± 0.8 (U)
JEMIMA-U(37.5)	Cylinder 26.7 cm dia	Repeated layers: 0.803 cm U(93.4) 1.204 cm U(nat)	18.88 (Av)	None	268.1 ± 1.3 (U)
U(16) assembly	Cylinder 38.1 cm dia core	Repeated layers: 0.304 cm U(93.36) 1.496 cm U(nat)	18.75 (Av)	U(nat), 19.0 g/cm^3 7.62 cm thick	683 ± 3.4 (U)

[a] A 0.293 cm gap between core and reflector.

Table 2. Specifications of spherical assemblies from Table 1 in a form convenient for calculation

Uranium assemblies:	Atoms/b cm					
	^{233}U	^{234}U	^{235}U	^{238}U	Critical radius (cm)	Reflector thickness (cm)[a]
LADY GODIVA	—	0.00049	0.04500	0.00250	8.741	—
FLATTOP-U(93)	—	0.00049	0.04449	0.00270	6.116	18.01
JEZEBEL-^{233}U	0.04671	0.00059	0.00001	0.00029	5.983	—
FLATTOP-^{233}U	0.04671	0.00059	0.00001	0.00028	4.137[b]	19.52
Plutonium assemblies:[c]	**Atoms/b cm**					
	^{239}Pu	^{240}Pu	^{241}Pu	^{242}Pu	Critical radius (cm)	Reflector thickness (cm)[a]
JEZEBEL-Pu(4.5)	0.03705	0.00175	0.00012	—	6.385	—
JEZEBEL-Pu(20.1)	0.02994	0.00788	0.00121	0.00016	6.599	—
FLATTOP-Pu	0.03674	0.00186	0.00012	—	4.533	19.60

[a] Reflector composition 0.00034 ^{235}U atoms/b cm, 0.04774 ^{238}atoms/b cm.
[b] A 0.293 cm gap between core and reflector.
[c] All plutonium contains 0.00138 Ga atoms/b cm.

Table 3. Spectral indexes of small metal assemblies

Assembly	$\bar{\sigma}_f(^{238}U)/\bar{\sigma}_f(^{235}U)$	$\bar{\sigma}_f(^{237}Np)/\bar{\sigma}_f(^{235}U)$	$\bar{\sigma}_f(^{239}Pu)/\bar{\sigma}_f(^{235}U)$
LADY GODIVA	0.165 ± 0.002	0.84 ± 0.01	1.40 ± 0.02
FLATTOP-U(93)	0.149 ± 0.002	0.76 ± 0.01	1.37 ± 0.02
JEZEBEL-Pu(4.5)	0.214 ± 0.003	0.96 ± 0.02	1.45 ± 0.03
JEZEBEL-Pu(20.1)	0.206 ± 0.003	0.92 ± 0.02	—
FLATTOP-Pu	0.180 ± 0.003	0.84 ± 0.01	—
JEZEBEL-^{233}U	0.213 ± 0.002	0.98 ± 0.02	—
FLATTOP-^{233}U	0.191 ± 0.003	0.89 ± 0.01	—

lifetime, ℓ, which is simply the ratio of reactivity to α. Table 5 gives values of α_{dc}, $(1-k_p)_{dc}=\overline{\gamma\beta}$, the effective delayed-neutron fraction, and ℓ for our various very-fast critical assemblies. In some cases, particularly for U-reflected systems, ℓ suffers from uncertainties in estimates of $\overline{\gamma\beta}$[21,23].

It should be noted that only limited selections from Tables 1 through to 5 can be used profitably for checking fast-reactor calculations. Because their utility is limited to high-energy processes, they provide no clues about important complications as the resonance region is approached.

2.2.2. *Reactivity calibrations.* Before leaving the small Los Alamos assemblies, consistency between two methods of calibrating their reactivity increments should be noted. Good comparisons were made possible by measurements extending as far as 80 cents above delayed criticality. Uniform increments of reactivity requiring calibration were provided by the linear portion of a control rod and by equal parts of fissile material at similar locations.

One method of calibration is the measurement of Rossi-α versus number of the uniform increments relative to delayed criticality. Because Rossi-α at prompt criticality is zero, the reactivity of one increment in dollars is simply the ratio of $\Delta\alpha$ per increment to α_{dc}.

The other method is the measurement of steady-state positive periods before and after a change of reactivity by a known number of increments. (Sensitivity is lost if periods are negative.) The well-known asymptotic solution of the kinetics equations relates period in seconds and reactivity in dollars in terms of delayed-neutron periods and abundances[24]. Keepin-Wimett delayed-neutron data provide the observed consistency with Rossi-α calibration[25].

Table 4. Central reactivity coefficients and ratios for small metal assemblies

Assembly	Reactivity coefficient ($\Delta k/k/g$ atom $\times 10^4$)						
	^{233}U	^{235}U	^{238}U	^{237}Np	^{239}Pu	^{240}Pu	^{10}B
LADY GODIVA	—	101 ± 1	16.2 ± 0.3	—	193 ± 2	115 ± 12	-38 ± 2
FLATTOP-U(93)[a]	232 ± 3[b]	133 ± 2	17.1 ± 0.6[b]	114 ± 2	253 ± 2	—	—
JEZEBEL-Pu(4.5)[c]	269 ± 3	158 ± 2	22.0 ± 0.4	163 ± 10	315 ± 3	205 ± 10	-49 ± 1
FLATTOP-Pu[d]	—	238 ± 3	14.5 ± 0.4	222 ± 3	452 ± 2	—	—
JEZEBEL-^{233}U	297 ± 3	—	41.7 ± 0.9	—	—	—	—
FLATTOP-^{233}U	401 ± 3	—	—	—	—	—	—
	Reactivity coefficient ratios						
	$^{233}U/^{235}U$	$^{238}U/^{235}U$	$^{237}Np/^{235}U$	$^{239}Pu/^{235}U$	$^{240}Pu/^{235}U$	$^{10}B/^{235}U$	
LADY GODIVA	—	0.160 ± 0.003	—	1.91 ± 0.03	1.14 ± 0.12	-0.38 ± 0.02	
FLATTOP-U(93)	1.74 ± 0.03	0.129 ± 0.005	0.86 ± 0.02	1.90 ± 0.03	—	—	
JEZEBEL-Pu(4.5)	1.70 ± 0.03	0.139 ± 0.003	1.03 ± 0.06	2.00 ± 0.03	1.30 ± 0.07	-0.31 ± 0.01	
JEZEBEL-Pu(20.1)[e]	—	—	—	1.99 ± 0.07	—	—	
FLATTOP-Pu	—	0.061 ± 0.001	0.93 ± 0.03	1.90 ± 0.03	—	—	

[a] Values for ^{238}Pu, ^{242}Pu and ^{241}Am are 225 ± 3, 120 ± 3 and 135 ± 1, respectively.
[b] From the equivalent Topsy assembly.
[c] The value for ^{241}Am is 207 ± 17.
[d] Values for ^{238}Pu, ^{242}Pu and ^{241}Am are 409 ± 6, 224 ± 4 and 280 ± 2, respectively.
[e] Only ratios are available: values for $^{238}Pu/^{235}U$ and $^{244}Cm/^{235}U$ are 2.01 ± 0.12 and 1.82 ± 0.10, respectively.

Table 5. Prompt-neutron characteristics of small metal assemblies

Assembly	$-\alpha_{dc}(\mu s^{-1})$	$\overline{\gamma\beta}(\times10^2)$	ℓ(ns)
LADY GODIVA	1.11 ± 0.02	0.645 ± 0.013	5.8
FLATTOP-U(93)	0.38 ± 0.01	0.665 ± 0.013	17.5
JEZEBEL-Pu(4.5)	0.64 ± 0.01	0.190 ± 0.004	3.0
FLATTOP-Pu	0.214 ± 0.005	0.276 ± 0.007	12.9
JEZEBEL-^{233}U	1.00 ± 0.01	0.289 ± 0.007	2.9
FLATTOP-^{233}U	0.267 ± 0.005	0.360 ± 0.009	13.5
JEMIMA-U(53)	0.63 ± 0.01	0.70[a]	11
JEMIMA-U(37.5)	0.46 ± 0.01	0.73[a]	16
U(16) assembly	0.175 ± 0.009	0.75[a]	43

[a] Computed value.

2.3. *Small metal assemblies elsewhere*

Outside Los Alamos most metal assemblies with homogeneous cores have been intended as fast-neutron sources. Argonne National Laboratory has its Fast Source Reactor, a TOPSY-like assembly, at Idaho, which serves as a steady-state source[26]. The others, pulsed after the manner of LADY GODIVA, are at Sandia Laboratories, Oak Ridge National Laboratory, Lawrence Livermore Laboratory, White Sands Missile Range and Aberdeen Proving Ground[27].

An exception, for the study of inherent characteristics, was RACHEL near Dijon, France. This assembly consisted of a near-spherical δ-phase plutonium core in a 9.3 cm thick natural uranium reflector, similar to FLATTOP-Pu, but with one half thickness reflector[28]. The quoted critical mass after corrections is 6.82 kg plutonium at 15.6 g/cm^3 plutonium density and 18.7 g/cm^3 uranium density[29].

Two other small metal assemblies had cores composed of plutonium rods. These were ZEPHYR at Harwell and BR 1/2 of the U.S.S.R. Atomic Energy Utilization Board. In the core of ZEPHYR, a roughly 15 cm equilateral cylinder, the rods (0.56 cm dia plutonium clad with nickel) were embedded in natural uranium. A typical critical mass was 14.7 kg ^{239}Pu with a 38 cm thick reflector of natural uranium rods about a solid column of uranium. Variations included a core of air-spaced rods packed more closely, and a reflector of graphite rods surrounding the uranium column. Quantities measured included neutron-flux distribution, spectral indexes and detailed spectra, and a large series of reactivity coefficients[30,31,32].

The BR-1 core consisted of air-spaced rods of 1 cm dia plutonium clad with stainless steel. The approximately 13 cm equilateral cylindrical core was surrounded by a 28.5 cm minimum thickness of depleted uranium or copper. The BR-2 reactor was similar but

with mercury filling the core lattice and uranium reflector blocks canned in stainless steel to permit operation as high as 200 kW. The critical mass was 12.2 kg ^{239}Pu as compared with 11.8 kg for the BR-1 version. After detailed neutronic measurements in BR-1 (as in ZEPHYR) BR-2 served as a source for the study of neutron propagation in a variety of materials[33,34].

The most recent fast assembly with a small rodded core is PURNIMA of Trombay, India[35]. The 3.5 L core contains air-spaced rods of 1 cm dia PuO_2 in 0.5 mm thick stainless steel. Inner reflectors of molybdenum (axial) and copper (radial) are surrounded by steel. This assembly mocks up the proposed Kalpakkam pulsed fast reactor, and is intended to establish the neutronic characteristics of that reactor.

3. FAST ASSEMBLIES WITH LARGER-VOLUME CORES

Our discussion of experiments with very-fast systems has been an historically convenient introduction to the principal body of this review. This part covers the much more comprehensive studies of fast assemblies with diluted cores, which may still be described simply. Core volume is a convenient parameter to distinguish between the two classes of assembly. The small metal critical assemblies listed in Table 1 have cores ranging in volume from 0.3 L to 36 L. For the category with diluted cores, the range is from 50 L to 4000 L.

One Los Alamos assembly, BIG TEN (125 L core), falls into the next category. Although it was not among the earliest of that group, it represents a transition from the small metal assemblies because it, too, is all metal without voids.

3.1. *BIG TEN*

BIG TEN is an all-uranium assembly consisting of a horizontal cylindrical core that averages U(10), surrounded by a depleted uranium reflector (Fig. 1)[36]. The advent of practical two-dimensional neutronic codes had reduced the desirability of a one-dimensional assembly. The core length has been adjusted to give 86 cents excess reactivity for kinetic measurements and 18 cents excess reactivity for spectral and material effectiveness measurements. The bulk of the core is interleaved plates of U(93) and natural uranium such that the average enrichment is 10% ^{235}U. But inserts of homogeneous U(10) permit measurements along the axis without influence of the heterogeneity. Table 6 gives a simplified description of BIG TEN, which is equivalent to a detailed two-dimensional description that appears in reference 36.

The spectral indexes of Table 7 are supplemented by detailed experimental spectra in reference 36.

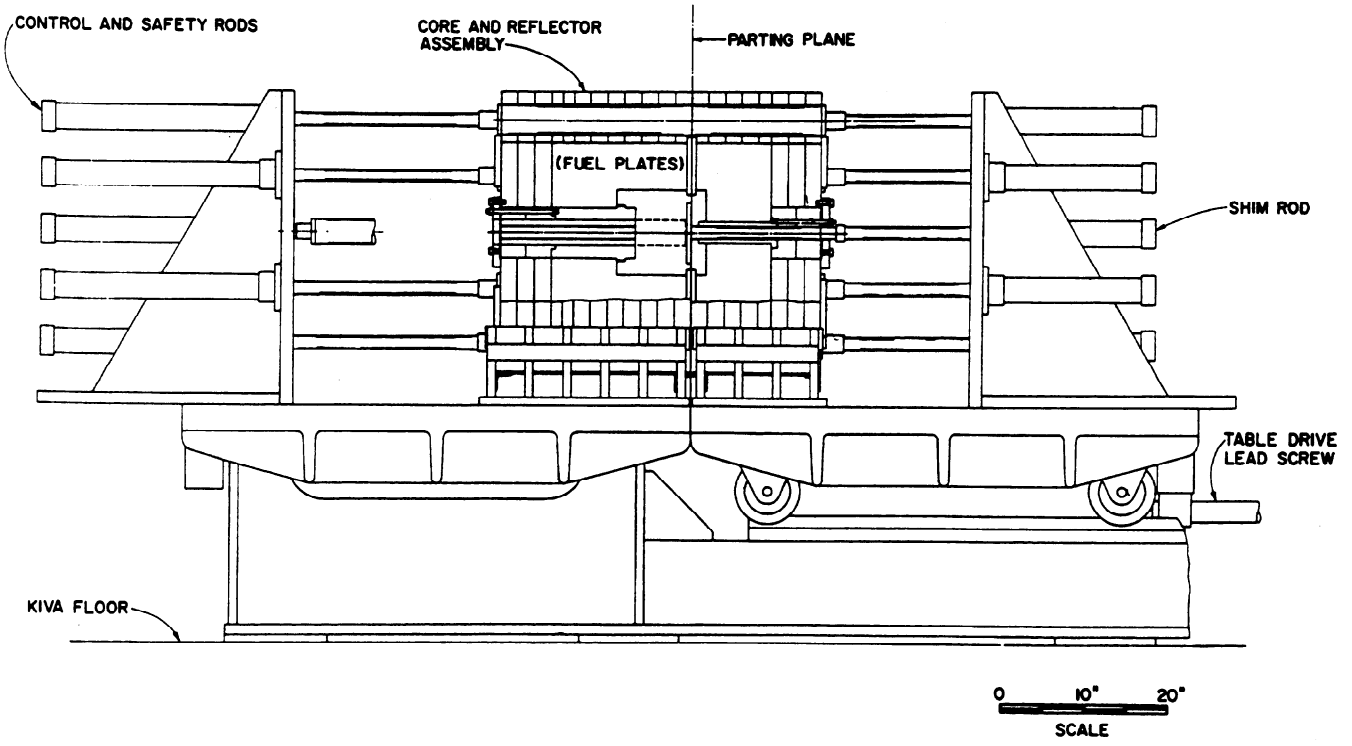

Fig. 1. The Big Ten Critical Assembly. Inserts of U(10) are surrounded by interleaved U(93) and natural uranium plates that average 10% ^{235}U.

Table 6. Simplified description of Big Ten

($k = 0.996 \pm 0.002$)	Core	Reflector
Radius (cm)	26.67	41.91
Half-length	27.94	48.26
^{234}U nuclei/b cm	0.00005	0.0
^{235}U nuclei/b cm	0.00484	0.00015
^{238}U nuclei/b cm	0.04268	0.04793

Table 7. Big Ten spectral indexes

Measured by the National Bureau of Standards

$$\bar{\sigma}_f(^{238}\mathrm{U})/\bar{\sigma}_f(^{235}\mathrm{U}) = 0.0373 \pm 0.0004$$
$$\bar{\sigma}_f(^{237}\mathrm{Np})/\bar{\sigma}_f(^{235}\mathrm{U}) = 0.316 \pm 0.005$$
$$\bar{\sigma}_f(^{239}\mathrm{Pu})/\bar{\sigma}_f(^{235}\mathrm{U}) = 1.18 \pm 0.02$$

Table 8. Central reactivity coefficients and ratios for Big Ten

Isotope	$\Delta k/k/(\text{g atom}) \times 10^5$	Ratio of ^{235}U coefficient
^{10}B	-73.9 ± 0.3	-0.512
^{232}Th	-15.1 ± 1.4	-0.105
^{233}U	249 ± 2	1.72
^{235}U	144.4 ± 0.7	
^{238}U	-7.35 ± 0.07	-0.051
^{237}Np	15.8 ± 0.9	0.109
^{238}Pu	157 ± 4	1.09
^{239}Pu	239.4 ± 1.4	1.66

Reactivity coefficients, selected from an extensive list in the reference, along with ratios, are given in Table 8.

Rossi-α data for BIG TEN, extending from -170 to 85 cents, are fit by the linear relationship

$$\alpha = -(1.17 \pm 0.01)(100 - \rho) \times 10^3 \text{ sec}^{-1},$$

where the reactivity ρ, in cents, is calibrated by positive-period measurements interpreted in terms of Keepin-Wimett delayed-neutron data. The delayed critical value $\alpha_{dc} = -1.17 \times 10^5 \text{ sec}^{-1}$ may be coupled with the effective delayed-neutron fraction $\beta_{eff} = 0.0072$, computed with ENDF/B-IV cross sections and Keepin-Wimett delayed-neutron yields. The ratio β_{eff}/α_{dc} gives the prompt-neutron lifetime 6.2×10^{-8} sec, only one order of magnitude greater than that of LADY GODIVA.

Most other simple diluted fast assemblies have been constituted of interleaved coupons of the reactor materials stacked in matrices of stainless steel or aluminium. A couple of exceptions are rodded assemblies more closely simulating power-reactor geometries.

3.2. *Diluted assemblies of the Argonne National Laboratory*

The greatest number of diluted assemblies that qualify as benchmarks are members of ANL's ZPR-3, ZPR-6 and ZPPR series. (ZPR represents 'zero-power reactor' and ZPPR 'zero-power plutonium reactor'.) The earliest to operate, the ZPR-3 assembly machine, and the latest, ZPPR, are in Idaho. The ZPR-6 machine is in Illinois.

3.2.1. *Measurement techniques*[37]. As the lengthy succession of ANL experiments progressed, techniques that have been discussed were refined and innovations were introduced. For measurement of a reactivity contribution an automatic transfer mechanism was repeatedly inserted into the assembly and withdrew a sample of the material of interest. Reactivity change was given by the motion of a calibrated servo control rod required to maintain constant power[38]. (This technique was borrowed for BIG TEN, the only LASL fast assembly large enough for a transfer mechanism.) The less precise, more tedious, manual introduction and removal of samples was used only for material replacements throughout a large region, such as required for the measurement of an overall sodium void coefficient.

An automatic transfer mechanism that carries a sample of fissionable material in an insulated heater is the most common device for measuring the Doppler coefficient of reactivity of the sample[39]. Increments of reactivity contribution over a range of temperature differences may be interpreted as Doppler coefficients, usually after correction for thermal expansion. This scheme was used first in the U.K. but adopted at ANL after earlier measurements with heated samples that remained in place[40].

Normally, ionization in gas-filled fission chambers gives internal fission rates or their ratios. Activities of irradiated foils, essential for establishing reaction rates of nonfissile materials, also may provide fission rates, though less conveniently. An alternative to measurement of fission-product activity of irradiated foils involves the use of solid-state track recorders[41,42]. Exposure of a material such as mica or polycarbonate resin against a fissionable foil generates fission-product tracks that can be counted at leisure.

Although a practice instead of technique, a program for exchanging fissionable foils has led to standardization by intercomparing the foil-weight determinations at various laboratories[43]. Further, a technique developed at Atomics International for measuring disintegrations of ^{10}B should be mentioned[44]. The number of disintegrations is established by precision

determination of the He released in the $^{10}B(n,\alpha)$ reaction. This technique has been used in Idaho, but not with the ANL assemblies that we are considering.

The technology of neutron spectrometry with internal proton-recoil proportional counters was perfected in ZPR assemblies[45]. The internal unit consists of a lead-shielded chamber and preamplifier. The shape of pulses from gamma rays that penetrate the lead provides a means of discrimination from proton-recoil pulses. A small amount of nitrogen with hydrogen or methane is used for calibration with 0.615 MeV protons from the reaction $^{14}N(n,p)$ induced by thermal neutrons. The hydrogen filling covers the low-energy portion, the combination giving remarkable detail.

3.2.2. *ZPR-3 assemblies.* The ZPR-3 machine is a split-table device with bundles of horizontal square aluminium or stainless-steel tubes (Fig. 2). Initially, core and reflector materials were plates of U(93), natural or depleted uranium, stainless steel, perforated aluminium, and sometimes graphite, generally 0.32 cm thick. The plates were interleaved in drawers of perforated stainless steel or aluminium which fit into the square tubes[46–48]. Later, there became available similar plates of plutonium, 0.64 cm thick plates of U-20% Pu, and cans of sodium and of carbonates and oxides (to simulate the oxygen in PuO_2 and UO_2)[49–51].

Several of the earliest ZPR-3 assemblies were parallelepipeds, four of the succeeding systems approximated spheres, and the others approximated cylinders. Most of the assemblies had thick reflectors of depleted uranium and stainless steel, some also containing aluminium. One series with constant composition demonstrated the dependence of critical size upon the ratio of cylinder height to diameter, and a number of assemblies mocked up reactors. Of the simpler systems, either spheres or near-equilateral cylinders, average compositions of core uranium ranged from U(9.4) to U(93). In one group of these, spectra were softened by adding graphite to give atomic ratios of C to ^{235}U ranging from about 3 to 12. In some of the later assemblies, Pu replaced ^{235}U as the fuel.

For comparison with calculation, it was necessary to correct the as-built assemblies for heterogeneity, irregular boundaries, and gaps between the parting surfaces[52]. Experimental bases for these corrections were provided by effects of varying the thickness of fuel plates, of substituting core material for reflector at various surface positions, and of changing gaps about the parting plane.

Of the 80 or so ZPR-3 assemblies, we have selected 12 of the simpler ones for idealization as homogeneous spheres or cylinders. These include five that have been chosen as benchmarks by the U.S. Cross Section Evaluation Working Group[53,54], the four spheres, representation of a broad range of core volumes and effective uranium enrichments, and two fueled with Pu.

For the 10 uranium assemblies, idealized critical dimensions are given in Table 9, atomic densities in Table 10, central spectral indexes in Table 11, central reactivity coefficient ratios for fissionable isotopes in Table 12, and Rossi-α data in Table 13[56]. Critical

Table 9. Dimensions of idealized ZRP-3 uranium assemblies[a]

Assembly	Shape	Approx. core volume (L)	Diameter (cm)	Length (cm)	Reflector thickness (cm)	
					Radial	Axial
6F	Sphere	51	46.0	—	30.5[b]	—
9A	Sphere	69	50.8	—	40.0[c]	—
12	Cylinder	103	53.1	46.3	38.9[c]	33.0[c]
11	Cylinder	142	59.1	51.9	36.2[c]	30.5[c]
36	Cylinder	142	50.1	72.0	~35.0[d]	35.5[d]
38	Sphere	319	82.8[e]	—	~35.0[d]	—
39	Sphere	410	92.2[e]	—	30.0[d]	—
25	Cylinder	459	86.7	77.7	40.8[c]	30.5[c]
29	Cylinder	477	91.5	72.5	30.5	30.5
34	Cylinder	594	93.0	87.5	34.9[d]	35.6[d]

[a] From references 47, 48 and 52 unless indicated otherwise.
[b] From reference 53, p. F7-2.
[c] From informal ANL reports.
[d] From ANL reports listed in Table 1 of reference 48.
[e] Fractional corrections from cylindrical assemblies of same composition (24 and 31, respectively).

Table 10. Compositions of idealized ZPR-3 uranium assemblies

Assembly	Core ^{235}U in U(%)	Atomic density (b^{-1} cm^{-1})[a,b] ^{235}U	^{238}U	^{234}U	Al	Fe	Cr	Ni	Mn	Si
6F	46.8	0.006726	0.00757	0.00007	0.01892	0.00764	0.00190	0.00083	0.00008	0.00009
9A	23.5	0.005622	0.01821	0.00006	0.01296	0.00884	0.00220	0.00096	0.00009	0.00010
12[c]	21.0	0.004517	0.01697	0.00005	—	0.00568	0.00141	0.00062	0.00006	0.00007
11	11.7	0.004565	0.03442	0.00005	—	0.00568	0.00141	0.00062	0.00006	0.00007
36[d]	15.9	0.004502	0.02375	0.00005	—	0.00789	0.00196	0.00086	0.00008	0.00009
38	9.4	0.003637	0.03501	0.00004	—	0.00578	0.00144	0.00063	0.00006	0.00007
39	39.0	0.002792	0.00434	0.00003	0.01410	0.01522	0.00379	0.00166	0.00016	0.00018
25	8.8	0.003421	0.03555	0.00003	—	0.00558	0.00144	0.00063	0.00006	0.00007
29[e]	33.2	0.002388	0.00477	0.00002	0.01470	0.01535	0.00382	0.00167	0.00016	0.00018
34[f]	31.2	0.002244	0.00493	0.00002	0.01537	0.01528	0.00380	0.00166	0.00016	0.00018

[a] Reflector atomic densities in b^{-1} cm^{-1} are 0.000091 ^{235}U, 0.04005 ^{238}U, 0.00454 Fe, 0.00113 Cr, 0.0050 Ni, 0.00005 Mn, 0.00005 Si, 6F only has additional 0.00137 Al.
[b] From references 47 and 48, assuming stainless steel composition of reference 53, p. F9-5.
[c] Also 0.02675 b^{-1} cm^{-1} carbon.
[d] Also 0.00400 b^{-1} cm^{-1} sodium.
[e] Also 0.01392 b^{-1} cm^{-1} oxygen.
[f] Also 0.00760 b^{-1} cm^{-1} carbon.

Table 11. Spectral indexes of selected ZPR-3 uranium assemblies[a]

Assembly	$\frac{\bar{\sigma}_f(^{233}U)}{\bar{\sigma}_f(^{235}U)}$	$\frac{\bar{\sigma}_f(^{239}Pu)}{\bar{\sigma}_f(^{235}U)}$	$\frac{\bar{\sigma}_f(^{240}Pu)}{\bar{\sigma}_f(^{235}U)}$	$\frac{\bar{\sigma}_f(^{234}U)}{\bar{\sigma}_f(^{235}U)}$	$\frac{\bar{\sigma}_f(^{236}U)}{\bar{\sigma}_f(^{235}U)}$	$\frac{\bar{\sigma}_f(^{238}U)}{\bar{\sigma}_f(^{235}U)}$
9A[b]	—	1.30[c]	—	0.45[c]	—	0.055[c]
12	1.46	1.10	—	0.30	—	0.048
11	1.51	1.17	—	0.31	—	0.038
36	1.46	1.19	0.35	0.32	0.100	0.044
38[b]	1.44	1.16	—	0.26	—	0.033
39[b]	1.52	1.18	0.33	0.35	0.112	0.048
25	—	1.17	—	0.26	—	0.032
29	1.47	1.06	0.30	0.27	0.087	0.038
34	1.46	1.07	0.28	0.26	0.080	0.037

[a] From reference 52 unless indicated otherwise.
[b] From cylindrical assembly of same composition (9, 24 and 31, respectively).
[c] From reference 47.

dimensions are corrected for core-surface irregularities, parting-plane gap, and heterogeneity. Characteristics of the two plutonium assemblies are grouped below with ZPR-6 and ZPPR systems.

Because of heterogeneity, both spectral indexes and reactivity coefficients are somewhat sensitive to the immediately surrounding structure. Although there was an attempt to make such measurements in representative regions, there remains some uncertainty in the appropriate computational modeling. To reduce uncertainty from this source only reactivity-coefficient ratios are given in Table 12. An additional complication with reactivity coefficients for the ZPR-3 assemblies considered above is the lack of correction to small-size samples in closely fitting cavities. Where sample sizes are available in the literature we have made such corrections based on the second-order perturbation theory[57].

Specifications here were obtained independently of reference 53, 'Cross Section Evaluation Working Group Benchmark Specifications', so may differ, usually in detail. But because there are significant differences for some of the reactivity-coefficients ratios, values from reference 53 appear in parentheses in Table 12.

3.2.3. *Large ANL assemblies.* Both the ZPR-6 and ZPPR assembly machines have much greater capacity

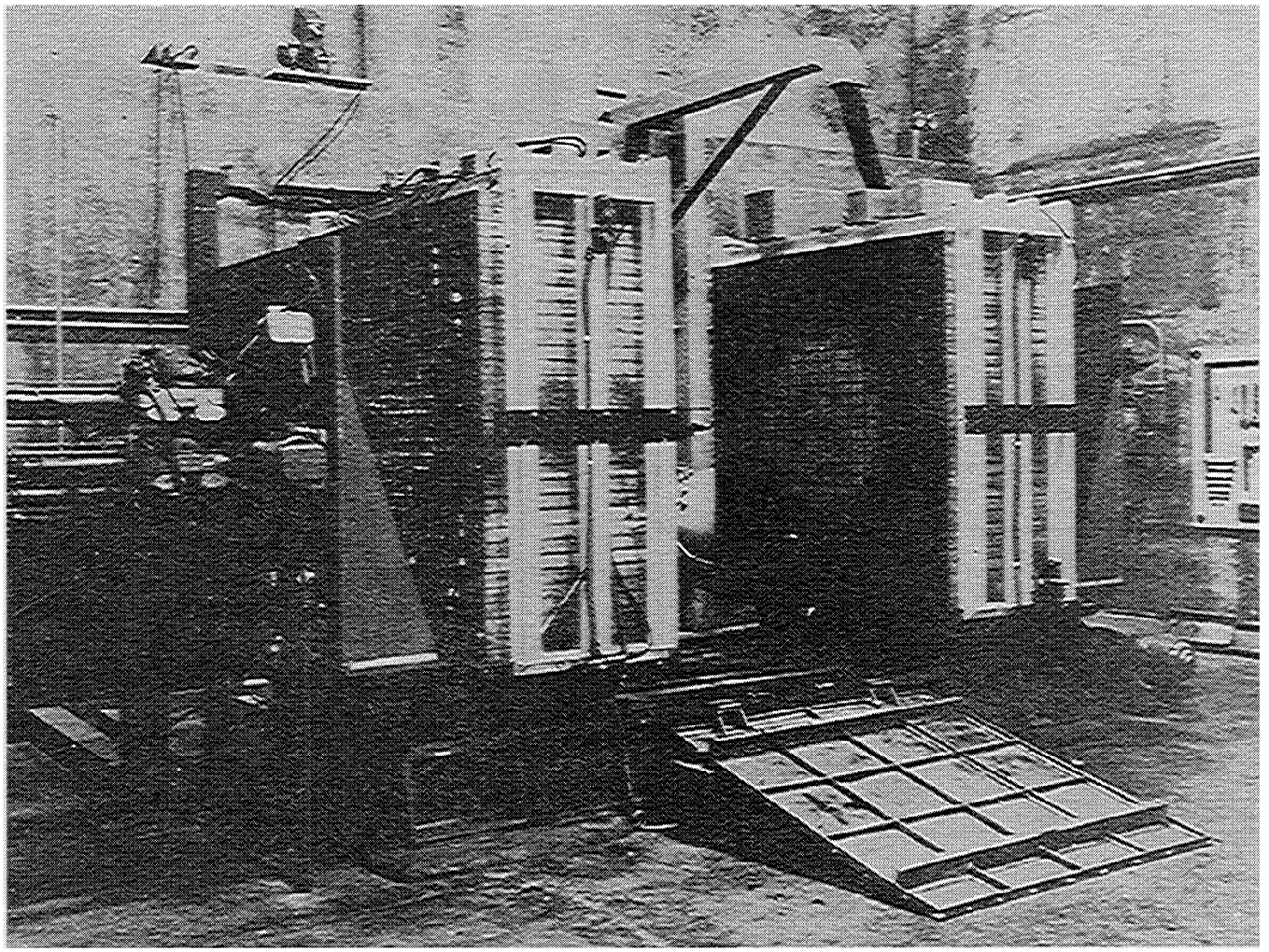

Fig. 2. The ZPR-3 Assembly Machine. Core and reflector components are inserted in the matrix of horizontal square tubes. (Courtesy Argonne National Laboratory.)

Table 12. Central reactivity coefficient ratios for selected ZPR-3 uranium assemblies[a]

Assembly	Reactivity coefficient ratios (Parenthetic values from reference 53)			
	$^{239}Pu/^{235}U$	$^{233}U/^{235}U$	$^{238}U/^{235}U$	$^{10}B/^{235}U$
12[a]	1.62[b]	1.83[c]	—	0.77[d]
	(1.60±0.05)	(1.71±0.5)	(−0.043±0.006)	—
11[a]	1.64[b]	1.78[c]	—	0.55[d]
	(1.70±0.06)	(1.80±0.05)	(−0.05±0.002)	(−0.59±0.02)
39[e]	1.74[f]	1.78[g]	−0.026[h]	—

[a] From reference 47.
[b] Estimated size correction factor 0.93.
[c] Estimated size correction factor 0.96.
[d] Estimated size correction factor 1.08.
[e] From cylindrical assembly 31 of same composition, reference 55.
[f] Estimated size correction factor 0.95.
[g] Estimated size correction factor 0.97.
[h] Estimated size correction factor 0.99.

Table 13. Delayed-critical Rossi-alpha values and prompt-neutron lifetimes for selected ZPR-3 assemblies[a]

Assembly	$\alpha_{dc}(\times 10^4\ S^{-1})$	Estimated β	$\ell(s \times 10^8)$
12	7.02±2%	0.0074	10.5
11	10.3±3%	0.0073	7.1
36	9.36±3%	0.0073	7.8
25	9.00±2%	0.0073	8.1
29	3.10±2%	0.0073	23.5
34	2.96±3%	0.0073	24.7

[a] From reference 56.

than ZPR-3. Hence they supported ANL benchmark assemblies with several-thousand-liter cores. Assemblies ZPR-6-6A and ZPR-6-7 have essentially single-zone cores and depleted uranium reflectors, and are fueled, respectively, with ^{235}U and Pu[58,59]. The Pu-fueled ZPPR-2 has a two-zone core and six-zone reflector, but is considered a benchmark system because it can be described in two dimensions. It is similar to ZPR-6-7 in effective composition and core size. This assembly is more complex than others we consider, so instead of reproducing its characteristics here, we refer the interested reader to its specifications in the benchmark listing of reference 53, or to descriptive ANL publications[58,59].

Of the two plutonium-fueled ZPR-3 assemblies that we group with ZPR-6-6A and 7, characteristics of ZPR-3-48 are developed much more satisfactorily in the literature[49]. In spite of its relatively deficient characterization[50,51], ZPR-3-56B is included because it had been chosen as a benchmark, primarily because of its Ni reflector[53].

Properties of ZPR-3-48 and 56B and of ZPR-6-6A and 7 are given in Tables 14–18, successively critical

Table 14. Critical dimensions of idealized plutonium-fueled and large uranium-fueled ZPR assemblies[a]

	ZPR-3-48	ZPR-3-56B	ZPR-6-6A	ZPR-6-7
Approx. core volume (L)	460	674	4420	3460
Core diameter (cm)	86.10	95.30[b]	188.9	166.8
Core length (cm)	79.02	94.50[b]	157.8	158.4
Axial refl. thickness (cm)	30.5	27.9[c]	34.2	34.3
Radial refl. thickness (cm)	34.5	34.2[c]	28.6	33.5

[a] From references 49, 50 and 58 pp. 86–101.
[b] Corrections for irregular surface, gap and heterogeneity are assumed proportionally the same as for ZPR-3-48.
[c] Radial reflector is the same radius as the core, axial reflector is full overall length.

Table 15. Composition of ZPR-6-6A[a]

Element (b^{-1} cm^{-1})	Core	Reflector (Av)
^{234}U	0.00001	—
^{235}U	0.001149	0.000086
^{238}U	0.0078	0.03955
O	0.01474	0.00002
Na	0.00920	—
Fe	0.01399	0.00447
Cr	0.00284	0.00125
Ni	0.00126	0.00054
Mn	~0.00010	~0.00004
Si	~0.00012	~0.00005
Mo	0.00001	—

[a] From reference 55, pp. 86–101.

dimensions, composition of ZPR-6-6A, composition of the plutonium-fueled assemblies, central spectral indexes, and central reactivity coefficients of fissionable isotopes. As before, dimensions are corrected for core-surface irregularities, gaps and inhomogeneity.

Except as noted in Table 17, central indexes of ZPR-6-6A and 7 are cell-averaged values obtained from mappings by irradiated foils. All central reactivity coefficients of Table 18 are corrected to zero sample size, those for ZPR-3-56B on the assumption that they are proportionately the same as for ZPR-3-48.

Most types of measurement beyond those tabulated above were made in ZPR-3-48, ZPR-6-7 and ZPPR-2. Radial and axial reaction-rate traverses of fissionable isotopes and ^{10}B are represented to some extent, as are similar reactivity-worth traverses of fissionable isotopes, ^{10}B, Na, Ta and stainless steel. The reactivity effect of Na removal in ZPPR-2, for example, is negative within about 82% of the core radius, and positive farther out.

Central Doppler effects of U (natural) O_2 and PuO_2 were measured in ZPR-3-48 and ZPPR, and in ZPR-6-7 were extended to $^{235}UO_2$, $^{233}UO_2$ and three mixtures of UO_2 and PuO_2. Both $^{235}UO_2$ and $^{233}UO_2$ showed an increase of reactivity with increasing temperature: for all others, there was a decrease. Within statistical uncertainty, the rate of change of reactivity with temperature, $\Delta\rho/\Delta T$, is proportional to 1/T. The equivalent proportionality of ρ and log T is shown in Fig. 3 for UO_2 in ZPR-3-48 and a $1PuO_2$-$2UO_2$ sample in ZPR-6-7.

Neutron-flux spectra, obtained with internal proton-recoil chambers for ZPR-3-48, ZPR-6-7 and ZPPR-2, extend from 1 or 1.5 keV to about 2 MeV. Figure 4 is an illustration. All the original spectra have similar irregularities, with the most pronounced depressions at 3 keV, 30 keV, and somewhat over 400 keV. The 3 keV depression and a smaller one at about 55 keV disappeared when sodium was removed from a region surrounding the spectrometer in

Table 16. Compositions of plutonium-fueled ZPR assemblies

	ZPR-3-48[a]		ZPR-3-56B[b]			ZPR-6-7[c]	
Element (b^{-1} cm^{-1})	Core	Reflector (av.)	Core	Axial refl.	Radial refl.[d]	Core	Reflector (av.)
^{239}Pu	0.001645	—	0.001328	—	—	0.000888	—
^{240}Pu	0.00011	—	0.00018	—	—	0.00012	—
^{241}Pu	0.000011	—	0.000025	—	—	0.000015	—
^{235}U	0.000016	0.000083	0.000014	—	—	0.000013	0.000086
^{238}U	0.00740	0.03969	0.00619	—	—	0.00580	0.03962
C	0.02077	—	0.00104	—	—	—	—
O	—	—	0.01519	—	—	0.01482	0.00002
Na	0.00623	—	0.00868	0.01346	0.00655	0.00913	—
Al	0.00011	—	—	—	—	—	—
Fe	0.01018	0.00492	0.01374	0.00882	0.00765	0.01353	0.00464
Cr	0.00253	0.00122	0.00249	0.00219	0.00189	0.00270	0.00130
Ni	0.00112	0.00054	0.00109	0.01948	0.04753	0.00121	0.00056
Mn	0.00011	0.00005	0.00010	0.00018	0.00029	0.00010	0.00003
Si	0.00012	0.00006	0.00012	0.00011	0.00012	0.00012	0.00004
Mo	0.00021	—	0.00034	—	—	0.00024	—

[a] From reference 49.
[b] From reference 50.
[c] From reference 58, pp. 86–101.
[d] Inner part weighted twice outer average.

Table 17. Central spectral indexes of plutonium-fueled and large uranium-fueled ZPR assemblies

Assembly	$\frac{\bar{\sigma}_f(^{233}U)}{\bar{\sigma}_f(^{235}U)}$	$\frac{\bar{\sigma}_f(^{239}Pu)}{\bar{\sigma}_f(^{235}U)}$	$\frac{\bar{\sigma}_f(^{240}Pu)}{\bar{\sigma}_f(^{235}U)}$	$\frac{\bar{\sigma}_f(^{234}U)}{\bar{\sigma}_f(^{235}U)}$	$\frac{\bar{\sigma}_f(^{236}U)}{\bar{\sigma}_f(^{235}U)}$	$\frac{\bar{\sigma}_f(^{238}U)}{\bar{\sigma}_f(^{235}U)}$
ZPR-3-48[a]	1.480±0.015	0.976±0.010	0.243±0.003	0.204±0.003	0.0670±0.0011	0.0307±0.0005
ZPR-3-56B[b]	1.478±0.015	1.028±0.010	0.282±0.003	0.195±0.002	0.0639±0.0006	0.0308±0.0003
ZPR-6-6A	—	0.98[c]	—	—	—	0.0219±0.0006[d]
ZPR-6-7[e]	—	0.942±0.011	~0.179	—	—	0.0223±0.0002

[a] From reference 49.
[b] Average from reference 51.
[c] From reference 59, pp. 21–27 by fission chambers.
[d] From reference 59, pp. 309–312, $\bar{\sigma}_{n,\gamma}(^{238}U)/\bar{\sigma}_f(^{235}U) = 0.138$.
[e] From reference 59, pp. 65–72, cell averages except ^{240}Pu ratio, $\bar{\sigma}_{n,\gamma}(^{238}U)/\bar{\sigma}_f(^{235}U) = 0.132$.

Table 18. Central reactivity coefficients of plutonium-fueled and large uranium-fueled ZPR assemblies[a]

Assembly	Reactivity coefficient ($\Delta k/k/g\text{-atom}) \times 10^4$ (Parenthetic values from reference 53 where difference is significant)				
	^{239}Pu	^{235}U	^{240}Pu	^{238}U	^{10}B
ZPR-3-48	10.8±0.1[b]	8.1±0.1	1.3[c]	−0.60±0.01	−9.10±0.06
ZPR-3-56B[d]	9.3±0.1	6.8±0.1	—	−0.40±0.01	−6.2±0.1
	(10.0±0.2)	(7.8±0.2)	—	(−0.50±0.02)	(−7.9±0.1)
ZPR-6-6A	3.04±0.11	2.18±0.03	—	−0.174±0.001	2.74±0.12
				(−0.187±0.0005)	(−2.93±0.13)
ZPR-6-7	3.76±0.05	3.11±0.07	0.7[e]	−0.26±0.01	−2.91±0.06

[a] From reference 59, pp. 309–312, unless noted otherwise.
[b] From reference 59, pp. 321–324.
[c] Uses data from reference 49.
[d] From reference 51, different conversion from Ih to Δk in reference 53.
[e] Uses data from reference 58, pp. 141–154.

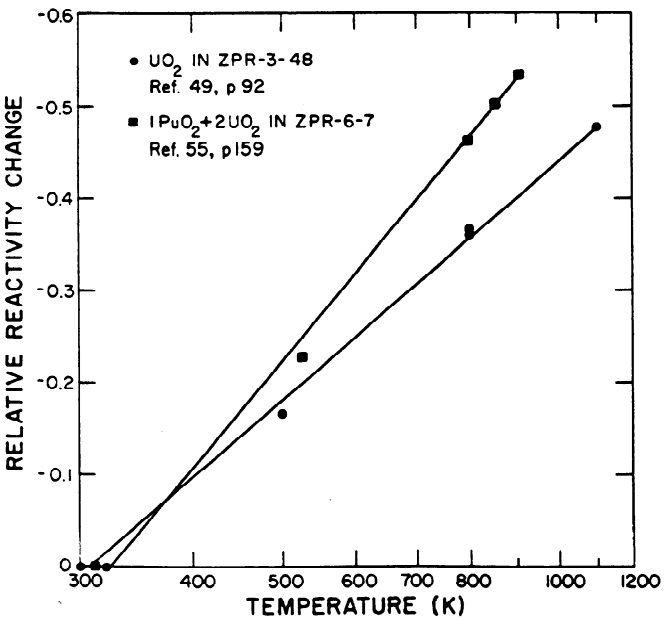

Fig. 3. Doppler coeffient data for two ANL assemblies. The proportionality of reactivity, ρ, and log T states that $\Delta\rho/\Delta T$ is proportional to T.

ZPPR-2, indicating that they are related to the 2.85 keV and 53 keV sodium scattering resonances. The 29 keV iron resonance and 440 keV oxygen resonance may account for the other most prominent depressions. More convincingly, however, the structures of measured spectra follow those of computed spectra faithfully.

For completeness, we should mention results of kinetic measurements in ZPPR-2. The value of effective delayed-neutron fraction, 0.341%, and of prompt-neutron lifetime, 59.0×10^{-8} sec, may be compared with the quantities listed in Table 5 for very fast assemblies.

Several ZPPR-3 assemblies are also categorized as benchmarks even though they are closer than ZPPR-2 to engineering mockups[60]. With an abundance of simple systems for checking basic nuclear parameters, it is natural that ANL emphasis be shifted to computationally difficult reactor features such as control elements and other perturbing structures.

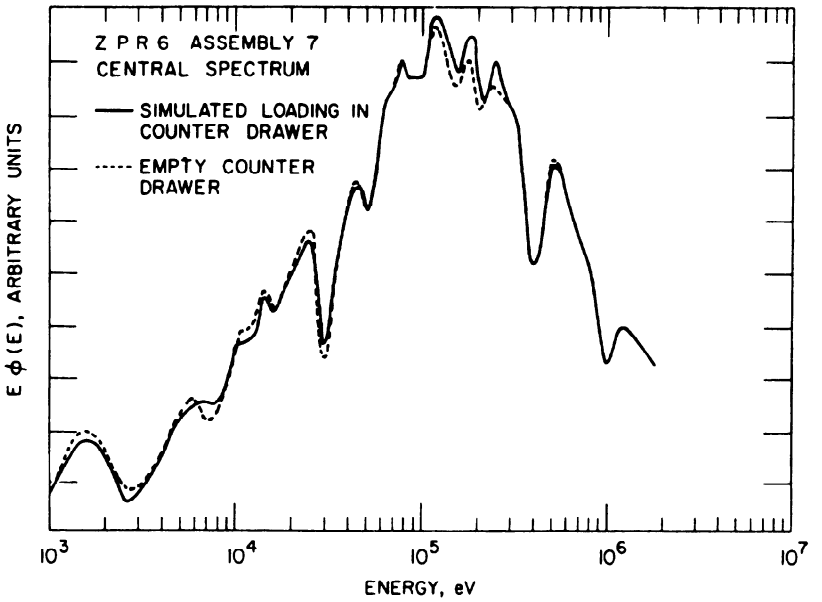

Fig. 4. Central neutron-flux spectra of a ZPR-6 assembly. Depressions at 3 and 55 keV are associated with sodium scattering resonances, and the 29 keV iron resonance and 440 keV oxygen resonance may account for the other most prominent depressions. (Courtesy Argonne National Laboratory.)

3.3. *Dilute assemblies of the United Kingdom*

Another large group of simple diluted systems consists of the VERA assemblies from Aldermaston and the ZEBRA assemblies from Winfrith[61–67]. (The acronyms represent Versatile Experimental Reactor Assembly, and Zero Energy Breeder Reactor Assembly.) All these assemblies approximate cylinders, and both enriched uranium and plutonium fuels are represented. (We exclude the plutonium-fueled QUAGGA assemblies at Dounreay because they have thermalizing graphite reflectors, and are either parallelepipeds or are taken beyond the fast-neutron regime by graphite moderation.)

Both the VERA and ZEBRA machines accommodate vertical fuel rods of square cross section (Fig. 5). Each rod is made up of plates of fuel, natural uranium and diluents stacked in a thin stainless-steel envelope. An advantage of the vertical arrangement is that much less containing material is required than with horizontal matrices and drawers. The fuel rods are positioned by fixtures at each end and, in ZEBRA, by light-weight intermediate spacers. VERA is a split-table machine that separates assemblies into halves. ZEBRA, however, is integral, relying upon control, safety and 'shutdown' rods that swing reactivity by at least 5%. A remote fuel-loading device minimizes the need to approach a shut-down assembly within thick concrete shielding.

The plates for the VERA core are 4.65 cm square, 0.32 cm thick for most U(93), 0.16 cm for the remainder, 0.26 cm plutonium clad in thin copper, 0.080 cm polyethylene, and 0.32 cm and 0.16 cm natural uranium and graphite[62]. The ZEBRA core plates are 5.1 cm square, and 0.16 cm thick for U(93) and 0.32 cm for plutonium in thin copper, U(37.5), natural uranium, stainless steel, aluminium and graphite, and 0.62 cm sodium in aluminium[65].

3.3.1. *VERA and ZEBRA Critical Parameters.* Of 13 simple critical assemblies on VERA, 10 were fueled with uranium at two average ^{235}U enrichments, and the others were fueled with plutonium. Four of the uranium assemblies differ only in shape, and several had no correction for heterogeneity. Of those fully corrected to homogeneous cylinders, we have selected three as typical: one with fuel averaging U(93), another averaging U(32), and the third with plutonium.

Four ZEBRA assemblies had single-zone cores and reflectors. The first duplicated a ZPR-3 system as part of a shakedown. We include the other three with those selected from VERA in tabulations of critical parameters: one with fuel averaging U(14) and the others with plutonium (Tables 19–23).

As for ANL assemblies, dimensions are adjusted to be appropriate for smooth, unperturbed, homogeneous cylinders. The reactivity-coefficient ratios of Table 23 are selected from a listing that includes hydrogen, boron enriched in ^{10}B, carbon, aluminium, iron and tantalum. Fission-rate traverses also are available. Another parameter not included in the tables is Rossi-α at delayed criticality. Values are $-(6.9\pm0.1)\times10^4$ sec^{-1} for VERA 1B, and $-(7.7\pm0.2)\times10^4$ sec^{-1} for VERA 3A[61]. From Rossi-α data, prompt-neutron lifetimes are estimated to be

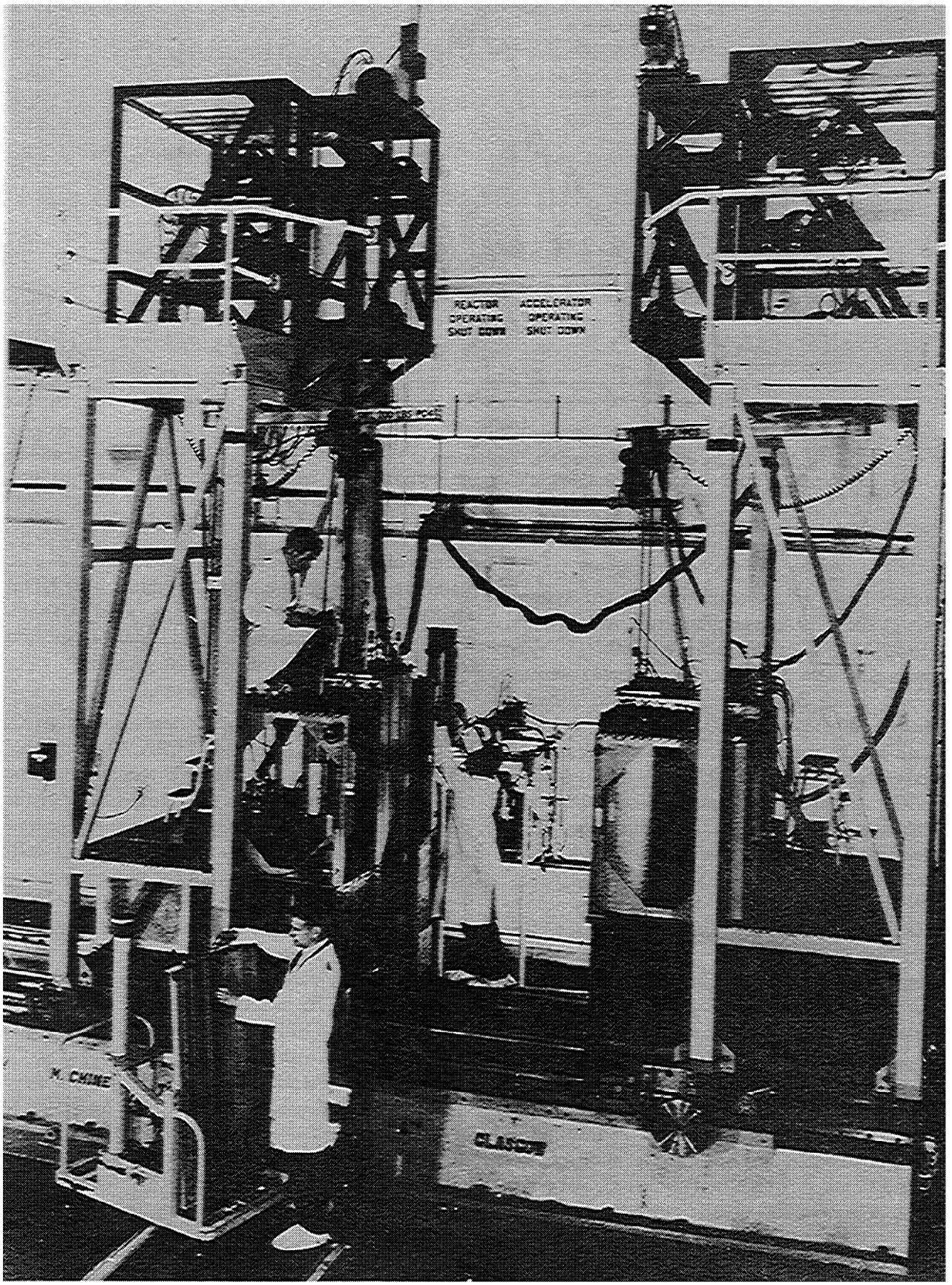

Fig. 5. VERA Reactor at Aldermaston. The two halves are separated for safe loading. Vertical tubes support core and reflector components. (Courtesy United Kingdom Atomic Energy Authority.)

Table 19. Critical dimensions of idealized VERA and ZEBRA cylinders

Assembly	Approx. core volume (L)	Diameter (cm)	Length (cm)	Reflector thickness (cm)	
				Radial	Axial
VERA-1B	31	38.2[a]	27.2[a]	39.4	36.4
VERA-3A	44	38.0[a]	38.7[a]	39.4	32.6
VERA-11A	12	26.5[a]	21.3[a]	45.0	41.2
ZEBRA-2[b]	424	80.3	83.8	30.5	30.5
ZEBRA-3[b]	58	46.0	34.9	30.5	30.5
ZEBRA-6A[c]	247	72.3	60.2	34.4	30.4

[a] Dimensions in reference 62, corresponding to raw critical masses given by ^{235}U or ^{239}Pu atom densities, are adjusted to yield corrected critical masses of reference 61.
[b] From reference 64.
[c] From reference 65.

Table 20. Compositions of VERA and ZEBRA uranium-fueled assemblies

Element (b^{-1} cm^{-1})	VERA-1B[a]		VERA-3A[a]		ZEBRA-2[b]	
	Core	Reflector	Core	Reflector	Core	Reflector
^{235}U	0.00735	0.00025	0.00619	0.00025	0.00251	0.00030
^{238}U[c]	0.00056	0.0344	0.01334	0.0344	0.0155	0.0410
H	0.000058	—	0.000148	—	—	—
C	0.0575	—	0.03577	—	0.0378	—
Fe	0.00628	0.00646	0.00628	0.00646	0.00384	0.00350
Cr	0.00164	0.00168	0.00164	0.00168	0.00100	0.00091
Ni	0.00069	0.00071	0.00069	0.00071	0.00039	0.00036

[a] From reference 62.
[b] From reference 64.
[c] Includes ^{234}U and ^{236}U.

Table 21. Compositions of VERA and ZEBRA plutonium-fueled assemblies

Element (b^{-1} cm^{-1})	VERA-11A[a]		ZEBRA-3[b]		ZEBRA-6A[c]	
	Core	Reflector	Core	Reflector	Core	Reflector
^{239}Pu	0.00721	—	0.00345	—	0.001879	—
^{240}Pu	0.00037	—	0.00020	—	0.00014	—
^{241}Pu	0.00003	—	0.00003	—	0.000016	—
^{235}U	—	0.00025	0.00023	0.00030	0.000046	0.00019
^{238}U	—	0.0344	0.03138	0.0410	0.00635	0.0268
C	0.0461	—	—	—	0.02959	0.0234
Na	—	—	—	—	0.00447	—
Al	—	—	—	—	0.00250	—
Fe	0.00607	0.00646	0.00420	0.00350	0.00426	0.00325
Cr	0.00158	0.00168	0.00110	0.00091	0.00127	0.00091
Ni	0.00066	0.00071	0.00043	0.00036	0.00044	0.00032
Cu	0.00796	—	0.00536	—	0.00083	—

[a] From reference 62, reference 53 lists 0.00045 b^{-1} cm^{-1} Ga in core.
[b] From reference 64.
[c] From reference 65.

Table 22. Central spectral indexes of VERA and ZEBRA assemblies[a]

Assembly	$\frac{\bar{\sigma}_f(^{233}U)}{\bar{\sigma}_f(^{235}U)}$	$\frac{\bar{\sigma}_f(^{239}Pu)}{\bar{\sigma}_f(^{235}U)}$	$\frac{\bar{\sigma}_f(^{240}Pu)}{\bar{\sigma}_f(^{235}U)}$	$\frac{\bar{\sigma}_f(^{237}Np)}{\bar{\sigma}_f(^{235}U)}$	$\frac{\bar{\sigma}_f(^{238}U)}{\bar{\sigma}_f(^{235}U)}$	$\frac{\bar{\sigma}_{n,\gamma}(^{238}U)}{\bar{\sigma}_f(^{235}U)}$
VERA-1B	1.50±0.03	1.10±0.02	0.41±0.02	0.39±0.02	0.068±0.001	0.132±0.005
VERA-3A	1.58±0.03	1.14±0.025	0.36±0.02	0.34±0.02	0.056±0.002	0.127±0.015
VERA-11A	1.49±0.03	1.07±0.02	0.475±0.02	0.43±0.02	0.077±0.002	—
ZEBRA-2	1.453±0.014	0.987±0.012	0.237±0.003	0.214±0.002	0.0320±0.0005	0.136±0.007
ZEBRA-3	1.542±0.019	1.190±0.014	0.373±0.005	0.353±0.005	0.0461±0.0008	0.111±0.005
ZEBRA-6A[b]	1.423±0.019	0.961±0.013	0.252±0.004	0.230±0.003	0.0364±0.0007	—

[a] From references 61 and 67 unless indicated otherwise.
[b] From references 65, which also gives $\bar{\sigma}_f(^{234}U)/\bar{\sigma}_f(^{235}U) = 0.209 \pm 0.003$, and $\bar{\sigma}_f(^{236}U)/\bar{\sigma}_f(^{235}U) = 0.072 \pm 0.002$.

Table 23. Central reactivity-coefficient ratios of VERA and ZEBRA assemblies

Assembly	$^{239}Pu/^{235}U$	$^{240}Pu/^{235}U$	$^{238}U/^{235}U$	$Na/^{235}U$
VERA-1B[a]	1.74±0.02	—	0.033±0.003	0.057±0.016
VERA-3A[a]	1.72±0.02	—	−0.021±0.001	0.028±0.007
VERA-11A[a]	1.81±0.03	—	0.013±0.001	—
ZEBRA-2[b]	1.42±0.02	0.27±0.03	−0.078±0.004	0.0022±0.0018
ZEBRA-3[b]	1.61±0.03	0.27±0.05	−0.050±0.002	−0.0127±0.0015
ZEBRA-6A[b]	1.44±0.02	—	−0.062±0.002	−0.0009±0.0004

[a] From reference 61, which includes absolute ^{235}U values.
[b] From reference 67.

9.5×10^{-8} sec for VERA 3A and 35×10^{-8} sec for VERA 11A[68].

U.K. spectral measurements represent great ingenuity and variety, but also include spectrometry with proton-recoil chambers similar to those of ANL[9]. Time-of-flight measurements with neutron beams extracted from pulsed subcritical assemblies extend experimental spectra to below 300 eV. With a 200 m flight path they overlap proton-recoil results to about 1 MeV.

The long flight path required with the relatively broad pulse of a multiplying assembly is reduced greatly in a double-scintillator spectrometer developed at Aldermaston. There the flight path is between a thin scintillator with photomultiplier in the external neutron beam and a thicker scintillator with photomultiplier, deviating from the beam by 45°. Timing is initiated by a proton-recoil pulse from the first scintillator and terminated by a near-coincident pulse in the second detector. In practice, this if the favored technique for neutron energies between 3–6 MeV, and ranks with use of an in-beam proton-recoil counter in the 1–3 MeV range. For these higher energies, the size of the proton-recoil chamber is increased considerably beyond the 4 cm i.d. that is appropriate for internal measurement.

Also attempted for this energy range were in-core measurements of alpha-plus-triton peak distribution in a ^6Li-semiconductor sandwich. There were problems with limited sensitivity and unfolding, but the difficulty that proves fatal is limited irradiation life.

Although inferred roughly from the temperature coefficient of reactivity in ZEBRA-2, there was no direct measurement of Doppler coefficient in any assembly we have listed. Instead, a succeeding ZEBRA assembly (No. 5) has a central heated region, comprising about 2% of the core volume, in which reactivity effects of temperature on a variety of internal structures can be determined. Some results are given in reference 67.

3.4. *FR0 at Studsvik*

The zero-energy assembly machine FR0 (Fast Reactor Zero) began operation in 1964 at Studsvik, Sweden[69]. It is a split-table machine with vertical elements, much like Aldermaston's VERA. Although the principal purpose was to gain experience with fast-reactor techniques, the first five FR0 assemblies could qualify as benchmarks. A limitation in the available quantity of U(20) fuel resulted in dense, small volume cores that serve primarily to confirm conclusions that can be drawn from ZPR-3 and VERA assemblies.

Three of these cores consisted of 87.7 vol% U(20) and 6.5 vol% stainless steel, one approximating a near-equilateral cylinder reflected by 35 cm thick Cu, another a cylinder reflected by ~12 cm thick natural uranium, and the other a sphere in 35 cm thick Cu. Core volumes were about 22, 30, and 21 L, respectively, smaller than other assemblies in the 'diluted' category. Spectra were softened in the other two cores, by replacing 29.2 vol% of the uranium with graphite in one case, and replacing another 7.5 vol% of the uranium with polyethylene in the other case. Core volumes were 51 and 39 L, and reflectors were 35 cm thick Cu. Structural perturbations were especially significant in the assembly that contained both graphite and polyethylene. At one stage, the assembly with polyethylene had a plutonium-fueled central zone of about 8 cm radius[70].

After correction for irregularities and heterogeneity, the spherical core has a critical radius of 17.2 cm and a composition in atoms/b-cm of 0.00851 ^{235}U, 0.03352 ^{238}U, 0.00408 Fe, 0.00096 Cr and 0.00048 Ni. The 35 cm thick reflector consists, in similar units, of 0.0748 Cu, 0.00408 Fe, 0.00096 Cr and 0.00048 Ni. Measured central spectral indexes for this assembly are $\bar{\sigma}_f(^{238}\text{U})/\bar{\sigma}_f(^{235}\text{U}) = 0.0583 \pm 0.014$, $\bar{\sigma}_f(^{237}\text{Np})/\bar{\sigma}_f(^{235}\text{U}) = 0.442 \pm 0.028$, $\bar{\sigma}_f(^{239}\text{Pu})/\bar{\sigma}_f(^{235}\text{U}) = 1.258 \pm 0.029$ and $\bar{\sigma}_f(^{238}\text{U})/\bar{\sigma}_{n,\gamma}(^{235}\text{U}) = 0.1044 \pm 0.0020$.

Data for other assemblies include central reactivity coefficients for a variety of elements, Rossi-α values, and results of Doppler measurements by activation of heated foils. Spectrometry by proton-recoil chambers was supplemented by 'sandwich-foil' techniques[69,70].

Further work with FR0 was intended to emphasize data relevant to steam-cooled fast reactors. This choice was dictated because of the emphasis elsewhere on sodium-cooled systems.

3.5. *Karlsruhe, Cadarache and cooperative programs*

The objective of a pair of ZPR-3 assemblies (Nos. 44 and 44A) was to provide guidance for the design of RAPSODIE at Cadarache, France. RAPSODIE is an experimental sodium-cooled fast reactor, operable at a power of 40 MW.

Broader cooperation led to a definition of the 'SCHERZO 556' core that we mentioned earlier. In spite of the French designation, this program was suggested in the U.K. and initiated with ZEBRA, but followed enthusiastically at Karlsruhe, Cadarache and Fontenay-aux-Roses, also in France[20]. Compositions averaging U(5.7) to U(6.5) with minimum structural material were set up as core inserts in ZEBRA, the SNEAK reactor at Karlsruhe, and the fast-thermal ERMINE reactor at Fontenay-aux-Roses, and as an exponential column at Cadarache. Cell reactivity worth values (or buckling in the exponential column) were used to arrive at the ^{235}U enrichment in undiluted uranium for which $k_\infty = 1$, and corresponding spectral indexes. Composite results are 5.56 ± 0.02 at% ^{235}U in uranium, i.e. U(5.49), $\bar{\sigma}_f(^{238}\text{U})/\bar{\sigma}_f(^{235}\text{U}) = 0.0227 \pm 0.0002$, and $\bar{\sigma}_{n,\gamma}(^{238}\text{U})/\bar{\sigma}_f(^{235}\text{U}) = 0.1154 \pm 0.0017$.

Similar measurements in the Japanese FCA reactor gave 5.57 ± 0.03 at% ^{235}U, $\bar{\sigma}_f(^{238}\text{U})/\bar{\sigma}_f(^{235}\text{U}) = 0.0220 \pm 0.0008$, $\bar{\sigma}_f(^{239}\text{Pu})/\bar{\sigma}_f(^{235}\text{U}) = 1.15 \pm 0.04$ and $\bar{\sigma}_f(^{237}\text{Np})/\sigma(^{235}\text{U}) = 0.23 \pm 0.01$[71]. Plutonium-uranium compositions led to $k_\infty = 1$ for about 4.0 at% fissile plutonium in ^{238}U + Pu.

Also, Japan participated with the U.K. in the MOZART project at Winfrith, directed toward designs of prototype fast reactors in both countries (MONJU in Japan, and PRF in the U.K.)[72]. The 18-month collaboration centered about three ZEBRA assemblies, all with plutonium fuel. The first and simplest, MZA, had a single-zone core but a five-zone breeder-reflector[73]. The core of the second, MZB, consisted of two zones, and the reflector was like that of MZA except that composition was varied in a 90° sector of one of the breeder zones. The other, MZC, was similar except that power-reactor-type control rods were installed in both core zones.

A high degree of cooperation is represented by the MASURCA assemblies and RAPSODIE at Cadarache and the SNEAK assemblies at Karlsruhe[74,75]. Fuel materials were exchanged between the two laboratories and there was common participation in experiments (the first of the MASURCA plutonium series was actually set up on the SNEAK machine). Further, the SNEAK program was coordinated with programs in the Benelux countries, all oriented toward development of the German-Benelux sodium-cooled fast-breeder SNR-300, to be located at Kalkar, Germany.

3.5.1. *Selected SNEAK assemblies.* Both MASURCA and SNEAK are vertical assembly machines, with rodded composition in MASURCA and stacked platelets in the later SNEAK assemblies (some of those earlier included MASURCA fuel rods). For our purpose, MASURCA and SNEAK may be considered as related to a single program, and we select four more nearly homogeneous SNEAK assemblies as representative[76,77]. All are of intermediate size. Two, identified as SNEAK-7A and 7B, with plutonium fuel and no sodium, have been chosen as ENDF benchmarks[53]. Of the others, which contain sodium,

SNEAK-9C-1 is fueled with enriched uranium, and SNEAK-9C-2 is fueled with plutonium.

The dimensions and compositions of these assemblies, Tables 24 and 25, differ from other presentations in that the entries are not adjusted to apply to idealized systems at criticality. Instead, average dimensions and compositions are retain and multiplication-factor increments are added to include corrections for heterogeneity and irregular shape, and built-in excess reactivity. The reason is that the corrections are computed in terms of Δk, not experimental. Thus the reference multiplication factors

Table 24. Dimensions of selected SNEAK assemblies

	Approx. core volume (L)	Diameter (cm)	Length (cm)
SNEAK-7A (k = 1.0055)[a]	113		
Inner core		31.72	44.04
Outer core		57.26	44.04
Reflector		117.26	105.04
SNEAK-7B (k = 1.0037)[a]	315		
Core		75.68	135.68
Reflector		70.06	131.06
SNEAK-9C-1 (k = 1.0022)[b]	266		
Inner core		38.82	59.96
Outer core		75.18	59.96
Reflector		137.26	120.92
SNEAK-9C-2 (k = 1.0054)[b]	247		
Inner core		38.82	60.04
Outer core		72.38	60.04
Reflector		137.26	121.00

[a] From reference 76.
[b] From reference 77.

Table 25. Compositions of selected SNEAK assemblies[a]

Element (b^{-1} cm^{-1})	SNEAK-7A (k = 1.0055)[b]		SNEAK-7B (k = 1.0037)[b]	SNEAK-9C-1 (k = 1.0022)[c]		SNEAK-9C-2 (k = 1.0054)[c,d]	
	Inner core	Outer core	Core	Inner core	Outer core	Inner core	Outer core
^{239}Pu	0.002637	0.002343	0.001831	—	—	0.001975	0.001735
^{240}Pu	0.00024	0.00021	0.00016	—	—	0.00018	0.00016
^{241}Pu	0.000022	0.000019	0.000015	—	—	0.000010	0.000009
^{235}U	0.000059	0.000296	0.000266	0.003078	0.003071	0.000044	0.000405
^{238}U	0.00796	0.00805	0.01458	0.00711	0.00708	0.00596	0.00608
H	—	—	0.000007	0.000024	0.000024	—	0.000003
C	0.02610	0.02554	0.00006	0.00309	0.00315	0.00005	0.00049
O	0.02185	0.02119	0.03319	0.01231	0.01216	0.01636	0.01570
Na	—	—	—	0.00886	0.00869	0.00833	0.00819
Al	0.00001	0.00119	0.00121	—	0.00038	0.00001	0.00044
Si	0.00009	0.00009	0.00014	0.00013	0.00013	0.00014	0.00015
Cr + Mn	0.00235	0.00236	0.00282	0.00285	0.00288	0.00303	0.00305
Fe	0.00797	0.00798	0.00980	0.01124	0.01119	0.01030	0.01036
Ni	0.00117	0.00118	0.00146	0.00233	0.00226	0.00166	0.00166
Mo + Nb	0.00003	0.00002	0.00003	0.00002	0.00002	0.00003	0.00003

[a] Reflector composition in b^{-1} cm^{-1}: 0.000162 ^{235}U, 0.03994 ^{238}U, 0.00001 C, 0.00005 Si, 0.00120 Cr + Mn, 0.00395 Fe, 0.00098 Ni, 0.00002 Mo + Nb.
[b] From reference 76.
[c] From reference 77.
[d] Also 0.000008 b^{-1} cm^{-1} ^{10}B.

are $k = 1.0055$ for SNEAK-7A, 1.0037 for 7B, 1.0022 for 9C-1 and 1.0054 for 9C-2. As for other assemblies, spectral indexes (Table 26), and central reactivity coefficients (Table 27) also are tabulated.

At both Cadarache and Karlsruhe, experimentally based values of material buckling are emphasized. For SNEAK assemblies 7A, 7B, 9C-1 and 9C-2, the quoted buckling values for core compositions are $(59.8 \pm 0.4) \times 10^{-4}$, $(34.83 \pm 0.07) \times 10^{-4}$, $(31.73 \pm 0.05) \times 10^{-4}$ and $(31.93 \pm 0.07) \times 10^{-4}$ cm^{-2}, respectively.

4. WHERE WE STAND

This completes our description of fast critical experiments. In general it goes beyond the ENDF compilation of benchmark assemblies[53]. The one exception is SEFOR, an experimental fast reactor that we excluded because of complexity. It provided valuable information about Doppler effects in a working environment.

The experimental data that we have summarized are primarily applicable to fast-reactor design, usually through an influence on multigroup cross-section sets. Some of these cross-section sets are proprietary, but examples referred to in the literature are CADARACHE of France and JAERI-FAST of Japan[78,79].

Less obvious, is the influence of integral data on the evaluated point cross-section sets, the UKNDL library of the U.K., KEDAK of Karlsruhe, SPENG of Sweden, ENDF/B of the U.S. and a U.S.S.R. library. Typically, these cross-section libraries have been based on differential data, with only informal guidance of

Table 26. Spectral indexes of selected SNEAK assemblies

	$\bar{\sigma}_f(^{238}U)/\bar{\sigma}_f(^{235}U)$	$\bar{\sigma}_f(^{239}Pu)/\bar{\sigma}_f(^{235}U)$	$\bar{\sigma}_{n,\gamma}(^{238}U)/\bar{\sigma}_f(^{235}U)$
SNEAK-7A[a]	0.0449 ± 0.0013	0.984 ± 0.029	0.138 ± 0.004
SNEAK-7B[a]	0.0328 ± 0.0006	0.975 ± 0.020	0.132 ± 0.004
SNEAK-9C-1[b]	0.0475 ± 0.0007	1.155 ± 0.035	0.129 ± 0.003
SNEAK-9C-2[b,c]	0.0463 ± 0.0006	1.104 ± 0.017	0.131 ± 0.003

[a] From reference 76.
[b] From reference 77.
[c] In SNEAK-9C-2: $\bar{\sigma}_f(^{240}Pu)/\bar{\sigma}_f(^{235}U) = 0.328 \pm 0.010$, $\bar{\sigma}_f(^{241}Pu)/\bar{\sigma}_f(^{235}U) = 1.32 \pm 0.04$, $\bar{\sigma}_f(^{241}Am)/\bar{\sigma}_f(^{235}U) = 0.285 \pm 0.012$.

Table 27. Central reactivity coefficients and ratios for SNEAK assemblies

	Reactivity coefficient ($\Delta k/k$/g-atom $\times 10^4$)					
Assembly	^{235}U	^{238}U	^{239}Pu	^{240}Pu	^{241}Pu	^{241}Am
SNEAK-7A[a]	19.1 ± 0.6	-0.99 ± 0.03	26.3 ± 0.8	6.4 ± 0.5	—	—
SNEAK-7B[a]	10.9 ± 0.2	-0.66 ± 0.01	15.2 ± 0.3	2.9 ± 0.3	—	—
SNEAK-9C-1[b,c]	8.0 ± 0.2	-0.32 ± 0.02	13.2 ± 0.5	2.6 ± 0.1	16.7 ± 0.8	—
SNEAK-9C-2[b]	9.9 ± 0.2	-0.35 ± 0.04	15.1 ± 0.4	3.1 ± 0.2	18.4 ± 0.7	-1.1 ± 0.2

	Reactivity coefficient ratios				
Assembly	$^{238}U/^{235}U$	$^{239}Pu/^{235}U$	$^{240}Pu/^{235}U$	$^{241}Pu/^{235}U$	$^{241}Am/^{235}U$
SNEAK-7A[a]	-0.051 ± 0.002	1.35 ± 0.06	0.33 ± 0.03	—	—
SNEAK-7B[a]	-0.060 ± 0.002	1.38 ± 0.04	0.26 ± 0.03	—	—
SNEAK-9C-1[b,c]	-0.040 ± 0.002	1.62 ± 0.07	0.31 ± 0.01	2.04 ± 0.11	—
SNEAK-9C-2[b]	-0.035 ± 0.002	1.50 ± 0.04	0.31 ± 0.02	1.80 ± 0.08	0.11 ± 0.01

[a] From reference 76.
[b] From reference 77.
[c] SNEAK-9C-2 sample-size corrections assumed.

data selection by integral information. There is some effort, however, to introduce integral data more systematically into the process of adjusting these point cross-section sets[80,81]. This effort promises increased significance of experimental fast-critical data.

Acknowledgements—This review was supported by the U.S. Department of Energy. It has benefited from the valuable advice of Gordon E. Hansen. Aubrey F. Thomas of the Atomic Weapons Research Establishment, Aldermaston and Adolf Garcia of the Argonne National Laboratory, Idaho, have kindly provided illustrations of critical assembly machines.

REFERENCES

1. White R. H. (1956) Topsy, A remotely controlled critical assembly machine, *Nucl. Sci. Eng.* **1**, 53–61.
2. Paxton H. C. (1976) Safety analysis of the Los Alamos critical experiments facility, Los Alamos National Laboratory report LA-6206, Vol. I.
3. Engle L. B., Hansen G. E. and Paxton H. C. (1960) Reactivity contributions of various materials in Topsy, Godiva and Jezebel, *Nucl. Sci. Eng.* **8**, 543–569.
4. Linenberger G. A. and Lowry L. L. (1954) Neutron detector traverses in the Topsy and Godiva critical assemblies, Los Alamos National Laboratory report LA-1653.
5. Grundl J. and Usner A. (1960) Spectral comparisons with high energy activation detectors, *Nucl. Sci. Eng.* **8**, 598–607.
6. Grundl J. A. (1967) A study of fission-neutron spectra with high-energy activation detectors—Part I. Detector development and excitation measurements, *Nucl. Sci. Eng.* **30**, 39–53.
7. Grundl J. A. (1968) A study of fission-neutron spectra with high-energy activation detectors—Part II. Fission spectra, *Nucl. Sci. Eng.* **31**, 191–206.
8. Byers C. C. (1960) Cross sections of various materials in the Godiva and Jezebel critical assemblies, *Nucl. Sci. Eng.* **8**, 608–614.
9. Sanders J. E., Burbidge B. H., Carter M. D., Hardiman J. P., Ingram G., Jowett D. and Sweet D. W. (1973) A review of Zebra techniques for the measurement of reactivity parameters, reaction rate ratios and spectra, *Proc. Int. Symposium on Physics of Fast Reactors*, Tokyo, October 16–19 (Power Reactor and Nuclear Fuel Development Corporation, 9–13, 1-chome Akasaka, Minato-ku, Tokyo) Vol. II, pp. 908–929.
10. Grundl J. A. and Hansen G. E. (1967) Measurements of average cross-section ratios in fundamental fast-neutron spectra, *Proc. Paris Conf. Nuclear Data for Reactors* (IAEA, Vienna) Vol. I, pp. 321–336.
11. Roberts J. H. and Kinney F. E. (1957) Measurements of Neutron Spectra by Use of Nuclear Emulsions Loaded with Li^6 Glass Specks, *Rev. Sci. Inst.* **28**, 610–615.
12. Kazanskii Yu. A., Belov S. P., Gurin V. N., Dmitrieva V. S., Doolin V. A., Efimenko V. F., Kuzin E. N., Lityaev V. M., Sokolov M. V. and Shapar A. V. (1973) Investigation of neutron spectra in fast critical assemblies, *Proc. Int. Symposium on Physics of Fast Reactors*, Tokyo, October 16–19 (Power Reactor and Nuclear Fuel Development Corporation, 9–13, 1-chome Akasaka, Minato-ku, Tokyo) Vol. II, pp. 930–944.
13. Dowdy E. J., Lozito E. J. and Plassmann E. A. (1975) The central neutron spectrum of the fast critical assembly Big-Ten, *Nucl. Technol.* **25**, 381–389.
14. Bendt P. J., Karr H. J. and Scott F. R. (1953) Alpha measurements on the Godiva critical assembly using a betatron, Los Alamos National Laboratory report LA-1515.
15. Orndoff J. D. (1957) Prompt neutron periods of metal critical assemblies, *Nucl. Sci. Eng.* **2**, 450–460.
16. Hansen G. E. and Paxton H. C. (1969) Reevaluated critical specifications of some Los Alamos fast-neutron systems, Los Alamos National Laboratory report LA-4208.
17. Stewart Leona (1960) Leakage neutron spectrum from a bare Pu^{239} critical assembly, *Nucl. Sci. Eng.* **8**, 595–597.
18. Wimett T. F. (1956) Time behavior of Godiva through prompt critical, Los Alamos National Laboratory report LA-2029.
19. Neuer J. J. and Stewart C. B. (1956) Preliminary survey of uranium metal exponential columns, Los Alamos National Laboratory report LA-2023.
20. Darrouzet M., Chandat J. P., Fischer E. A., Ingram G., Sanders J. E. and Scholtyssek W. (1973) Studies of Unit k lattices in metallic uranium Assemblies Zebra 8H, Sneak 8, Ermine and Harmonie U.K., *Proc. Int. Symposium on Physics of Fast Reactors*, Tokyo, October 16–19 (Power Reactor and Nuclear Fuel Development Corporation, 9–13, 1-chome Akasaka, Minato-ku, Tokyo) Vol. I, pp. 537–570.
21. Hansen G. E. (1961) Status of computational and experimental correlations for Los Alamos fast-neutron critical assemblies, *Proc. IAEA Seminar Physics of Fast and Intermediate Reactors*, Vienna, August 3-11, IAEA, Vienna (1962), Vol. I, pp. 445–455.
22. Hansen G. E., private communication.
23. Keepin G. R. (1965) *Physics of Nuclear Kinetics*, Addison Wesley Publishing Co., Reading, MA, p. 180.
24. ibid., Chapter 7.
25. Keepin G. R., Wimett, T. F. and Zeigler R. K. (1957) Delayed neutrons from fissionable isotopes of uranium, plutonium and thorium, *Phys. Rev.* **107**, 1044–1049.
26. Brunson G. S. (1959) Design and hazards report for the Argonne Fast Source Reactor (AFSR), Argonne National Laboratory report ANL-6024.
27. Long R. L. (1976) Status of fast pulse reactors in the U.S.A., *Proc. U.S./Japan Seminar on Fast Pulse Reactors*, Tokyo, January 19–23, Nuclear Engineering Research Laboratory, University of Tokyo, Tokai, pp. 9–16.
28. Bourgeois P., Clair C., Comte R. and Long J. J. (1961) Description de l'Assemblage Critique RACHEL, Proc. IAEA Seminar Physics of Fast and Intermediate Reactors, Vienna, August 3–11, IAEA, Vienna (1962), Vol. I, pp. 313–319.
29. Clair C., Propriétés neutroniques de l'Assemblage critique RACHEL, ibid., pp. 321–325.
30. Holmes J. E. R., McVicar D. D., Rose H., Smith R. D. and Shepherd L. R. (1955) Experimental studies on fast neutron reactors at AERE, *Proc. Int. Conf. Peaceful Uses At. Energy*, 1st, Geneva, United Nations, New York (1956), Vol. 5, pp. 331–341.
31. Smith R. D. and Sanders J. E. (1958) Experimental work with Zero Energy Fast Reactors, *Proc. Int. Conf. Peaceful Uses At. Energy*, 2nd, Geneva, United Nations, New York (1958), Vol. 12, pp. 89–118.

32. *Directory of Nuclear Reactors, Vol. III, Research, Test and Experimental Reactors*, IAEA, Vienna, (1960), pp. 337–338.
33. Leipunsky A. I., Abramov A. I., Andreev V. N., Baryshnikov A. I., Bondarenko I. I., Fetisov N. I., Galkov V. I., Golubev V. I., Gulko A. D., Guseinov A. G., Kazachkovsky O. D., Kozlova N. V., Krasnoyavov N. V., Kuzminov B. D., Morozov V. M., Nikolaev M. N., Sherman L. E., Smirenkin G. N., Savissky Iu. Ya., Ukraintsev F. I. and Usachev L. N., (1958) Studies in the Physics of Fast Neutron Reactors, Proc. Int. Conf. Peaceful Uses At. Energy, 2nd, Geneva, United Nations, New York (1958), Vol. 12, pp. 3–15.
34. *Directory of Nuclear Reactors, Vol. III, Research, Test and Experimental Reactors*, IAEA, Vienna (1960), pp. 341–348.
35. Iyengar P. K., Basu T. K., Chandramoleschwar K., Das S., Job P. K., Kapil S. K., Nargundkar V. R., Pasupathy C. S., Srinivasan M. and Subba Rao K. (1979) PURNIMA—A PuO_2-fueled Zero-Energy Fast Reactor at Trombay, *Nucl. Sci. Eng.* **70**, 37–52.
36. Hansen G. E. and Paxton H. C. (1979) A critical assembly of uranium enriched to 10% in uranium-235, *Nucl. Sci. Eng.* **72**, 230–236.
27. Davey W. G. and Redman W. C. (1970) *Techniques in Fast Reactor Critical Experiments*, Gordon and Breach Science Publishers, New York.
38. Bennett E. F. and Long R. L. (1963) Precision limitation in the measurement of small reactivity changes, *Nucl. Sci. Eng.* **17**, 425–432.
39. Fisher G. J., Meneley D. A., Hwang R. N., Groh E. F. and Till C. E. (1966) Doppler effect measurements in plutonium-fueled fast power breeder reactor spectra, *Nucl. Sci. Eng.* **25**, 37–46.
40. Greebler P. and Pflasterer G. R. (1966) Doppler and sodium void reactivity effects in fast reactors, *Reactor Physics in the Resonance and Thermal Regions*, MIT Press, Cambridge, Vol. II, pp. 343–370.
41. Gold R., Armani R. J. and Roberts J. H. (1968) Absolute fission rate measurements with solid-state track detectors, *Nucl. Sci. Eng.* **34**, 13–32.
42. Roberts J. H., Huang S., Armani R. J. and Gold R. (1968) Fission rate measurements in low-power fast critical assemblies with solid-state track recorders, *Nucl. Appl.* **5**, 247–252.
43. Amundson P. I., Broomfield A. M., Davey W. G. and Stevenson J. M. (1966) An international comparison of fission detector standards, *Proc. Int. Conf. Fast Critical Experiments and their Analysis*, October 10–13, ANL-7320, pp. 679–687.
44. Farrar H. and Lippincott E. P. (1977) Helium production measurements for neutron dosimetry and damage correlations, Proc. 2nd ASTM-Euratom Symposium on Reactor Dosimetry: Dosimetry Methods for Fuels, Cladding and Structural Materials, Palo Alto, October 3–7, NUREG/CP-004, Vol. 2, pp. 725–738.
45. Bennett E. F. and Yule T. J. (1971) Techniques and analyses of fast-reactor neutron spectroscopy with proton-recoil proportional counters, Argonne National Laboratory report ANL-7763.
46. Cerutti B. C., Lichtenberger H. V., Okrent D., Rice R. E. and Thalgott F. W. (1956) ZPR-III, Argonne's fast critical facility, *Nucl. Sci. Eng.* **1**, pp. 126–134.
47. Long J. K., Loewenstein W. B., Branyan C. E., Kirn F. S., Okrent D., Rice R. E. and Thalgott F. W. (1958) Fast neutron power reactor studies with ZPR-III, Proc. Int. Conf. Peaceful Uses Atomic Energy, 2nd, Geneva, United Nations, New York (1958), Vol. 12, pp. 119–141.
48. Thalgott F. W., Long J. K., Davey W. G., Kato W. Y., Carpenter S. G., Morewitz H. A. and Best G. H. (1964) Fast critical experiments and their analysis, Proc. Int. Conf. Peaceful Uses of Atomic Energy, 3rd, Geneva, United Nations, New York (1965), Vol. 6, pp. 124–136.
49. Broomfield A. M., Hess A. L., Amundson P. I., Baird Q. L., Bennett E. F., Davey W. G., Gasidlo J. M., Keeney W. P., Long J. K. and McVeen R. L. (1970) ZPR-III assemblies 48, 48A and 48B: The study of a dilute plutonium-fueled assembly and its variants, Argonne National Laboratory report ANL-7759.
50. Reactor Development Program Progress Report, March (1969), Argonne National Laboratory report ANL-7561, pp. 8–15.
51. Reactor Development Program Progress Report, April-May (1969), Argonne National Laboratory report ANL-7577, pp. 17–35.
52. Davey W. G. (1964) An analysis of 23 ZPR-III fast reactor critical experiments, *Nuc. Sci. Eng.* **19**, pp. 259–273.
53. Cross section evaluation working group benchmark specifications, Brookhaven National Laboratory report BNL-19302 (ENDF 202) (1974).
54. Hardie R. W., Schenter R. E. and Wilson R. E. (1975) An analysis of selected fast critical assemblies using ENDF/B-IV neutron cross sections, *Nucl. Sci. Eng.* **57**, pp. 222–238.
55. Palmedo P. F. Editor (1971) Compilation of fast reactor experiments, Brookhaven National Laboratory report BNL-15746, Vol. I, p. 4.1-*1*-31.
56. Brunson G. S., Curran R. N., Gasidlo J. M. and Huber R. J. (1963) A survey of prompt-neutron lifetimes in fast critical systems, Argonne National Laboratory report ANL-6681.
57. Hansen G. E. and Maier C. (1960) Perturbation theory of reactivity coefficients for fast-neutron critical systems, *Nucl. Sci. Eng.* **8**, 532–542.
58. Applied Physics Division Annual Report, 1 July 1970–30 June 1971, Argonne National Laboratory report ANL-7910, pp. 86–101, 117–131, 141–154, 156–169, 228–238, 241–249, 265–270.
59. Applied Physics Division Annual Report, 1 July 1971–30 June 1972, Argonne National Laboratory report ANL-8010, pp. 21–27, 65–73, 154–162, 164–171, 280–282, 309–312, 321–324.
60. Amundson P. I., Bennett E. F., Carpenter S. G., Kato W. Y., LeSage L. G., Lewis R. A., Palmer R. G., Till C. E., Travelli A. and Zolotar B. A. (1973) U.S. fast integral experiments program, *Proc. Int. Symposium on Physics of Fast Reactors*, Tokyo, 16–19 October, Power Reactor and Nuclear Fuel Development Corporation, 9–13, 1-chome Akasaka, Minato-ku, Tokyo, Vol. I, pp. 431–463.
61. Smith R. D., Rowlands J. L., Baker A. R., Smith D. C., Hicks E. P., Mann J. E. and Weale J. (1964) Fast reactor physics, including results from U.K. Zero Power Reactors, *Proc. Int. Conf. Peaceful Uses of Atomic Energy*, 3rd, Geneva, United Nations, New York (1965), Vol. 6, pp. 90–102.
62. Weale J. W., McTaggart M. H., Goodfellow H. and Paterson W. J. (1963) Operating experience with the Zero-Energy Fast Reactor VERA, *Proc. Symposium on Exponential and Critical Experiments*, Amsterdam, September 2–6, IAEA, Vienna (1964), Vol. I, pp. 159–195.
63. Smith R. D. (1962) ZEBRA—A Zero-Power Fast Reactor, *Nucl. Eng.* **7**, pp. 364–367.

64. Thalgott F. W., Baker A. R. and Carpenter S. G. (1965) Critical assemblies, *Proc. Topical Meeting Fast Reactor Technology*, Detroit, 26–28 April, American Nuclear Society publication ANS-100, pp. 225–243.
65. Adamson, J., Absalom R. M., Baker A. R., Ingram G., Pattenden S. K. I. and Stevenson J. M. (1966) ZEBRA 6: A dilute plutonium-fueled assembly, *Proc. Int. Conf. on Fast Reactor Experiments and Their Analysis*, Argonne, 10–13 October, Argonne National Laboratory report ANL-7320, pp. 216–230.
66. From informal U.K. report.
67. Smith R. D., Baker A. R. and Rowlands J. L., (1966) Theoretical and experimental work on the physics of fast reactors, *Proc. British Nuclear Energy Society Conf. Fast Breeder Reactors*, London, 17–19 May, Pergamon Press, London (1967), pp. 513–543.
68. Brunson, G. S. (1975) On the possible connection between the central worth discrepancy and the dollar discrepancy, *Nucl. Inst. and Methods*, **125**, 139–147.
69. *Proc. Int. Conf. on Fast Reactor Experiments and Their Analysis*, Argonne, 10–13 October 1966, Argonne National Laboratory report, ANL-7320; Andersson T. L., Björéus L., Hellstrand E., Häggblom H., Londen S.-O. and Tirén L. I., Experimental and theoretical work at the Zero-Energy Fast Reactor FR0, pp. 159–185; and Bergström A., Brunfelter B., Kockum J. and Söderberg S., Pulsed-source, Rossi-α and variance-to-mean measurements performed at the FR0 reactor, pp. 694–705.
70. Andersson T. L. and Qazi M. N. (1970) Measurement of the neutron spectra in FR0 cores 5, 9 and PuB-5 using resonance sandwich detectors, Studsvik report AE-392.
71. Iijima T. and Mukaiyama T. (1973) Evaluation of fission spectra and cross sections by zero-leakage core experiments, *Proc. Int. Symposium on Physics of Fast Reactors*, Tokyo, 16–19 October, Power Reactor and Nuclear Fuel Development Corporation, 9-13, 1-chome Akasaka, Minato-ku, Tokyo, Vol. I, pp. 520–536.
72. Campbell, C. G., Sanders J. E., Rowlands J. L. and Kobayashi S. The scope of the MOZART programme and the general conclusions drawn from it, ibid., Vol. I, pp. 259–268.
73. Ingram G., Stevenson J. M., Smith R. W., Ichimori T. and Konishi T. Critical size and central reactor rate results from the MOZART programme and their predictions, ibid., Vol. I, pp. 269–288.
74. Barré, J. Y., Boyer J., Mougniot J. C. and Sicard B. (1972) Reactor physics and fast power breeders: Masurca core R-Z program, Proc. Ntl. Topical Meeting on New Developments in Reactor Physics and Shielding, Kiamesha Lake, 12–15 September, U.S. AEC CONF-720901, Book 2, pp. 822–838.
75. Fischer E. A. and Kusters H. (1973) The fast reactor physics program in the Federal Republic of Germany, *Proc. Int. Symposium on Physics of Fast Reactors*, Tokyo, 16–19 October, Power Reactor and Nuclear Fuel Development Corporation 9–13, 1-chome Akasaka, Minato-ku, Tokyo, Vol. I, pp. 36–60.
76. Fischer E. A. and McGrath P. E. (1974) Physics investigations of two Pu-fueled fast critical assemblies: SNEAK-7A and 7B, Kernforschungszentrum Karlsruhe report KFK 1939.
77. Scholtyssek W. (1977) Physics investigations of sodium-cooled fast reactors: SNEAK-Assembly 9C, Kernfurschungszentrum Karlsruhe report KFK 2361.
78. Chaudat J. P., Barré J. Y. and Khairallah A. (1973) Improvements of the predicted characteristics for fast power reactor from integral experiments: Cadarache Version III multigroup cross section set, *Proc. Int. Symposium on Physics of Fast Reactors*, Tokyo, 16–19 October, Power Reactor and Nuclear Fuel Development Corporation, 9–13, 1-chome Akasaka, Minato-ku, Tokyo, Vol. III, pp. 1207–1238.
79. Katsuragi, S., Takano H., Hasegawa A., Suzuki T. and Kikuchi Y. Developments of the JAERI calculation systems for fast reactors, ibid., Vol. III, pp. 1117–1132.
80. Usachev L. N., Kazanskij Yu. A., Dulin V. A. and Bobkov Yu. G. Adjustment of evaluated microscopic data on the basis of evaluated integral experiments: International Atomic Energy Agency document INDC(CCP)-109/U, translated August 1977.
81. Weisbin C. R., Marable J. H., Collins P. J., Cowan C. L. Peelle R. W. and Salvatores M. (1979) Specifications for adjusted cross section and covariance libraries based upon CSEWG fast reactor and dosimetry benchmarks, Oak Ridge National Laboratory document ORNL-5517.